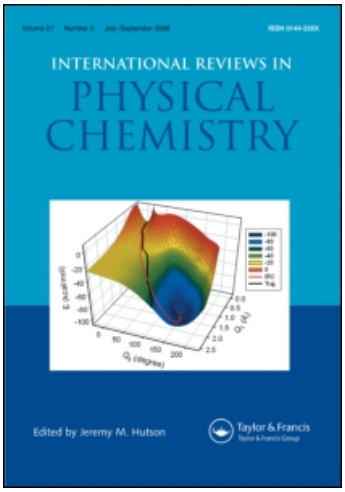

International Reviews in Physical Chemistry
Publication details, including instructions for authors and subscription information:
http://www.informaworld.com/smpp/title~content=t713724383

Main group metal-ligand interactions in small molecules: New insights from laser spectroscopy

Andrew M. Ellis

Online publication date: 26 November 2010

To cite this Article Ellis, Andrew M.(2001) 'Main group metal-ligand interactions in small molecules: New insights from laser spectroscopy', International Reviews in Physical Chemistry, 20: 4, 551 — 590
To link to this Article: DOI: 10.1080/01442350110062542
URL: http://dx.doi.org/10.1080/01442350110062542

INT. REVIEWS IN PHYSICAL CHEMISTRY, 2001, VOL. 20, NO. 4, 551–590

Main group metal–ligand interactions in small molecules: new insights from laser spectroscopy

ANDREW M. ELLIS†

Department of Chemistry, University of Leicester, University Road, Leicester LE1 7RH, UK

The application of laser electronic spectroscopy to small metal-containing molecules, composed of a single metal atom bound to a single molecular ligand, is reviewed. The focus is on recent studies performed using supersonic cooling and is illustrated by selected examples containing group 2 (Mg, Ca, Sr and Ba) or group 12 metals (Zn and Cd). The discussion emphasizes similarities and differences in the electronic structures of these molecules as deduced from their spectra and from supporting theoretical calculations.

Contents

† e-mail address: andrew.ellis@le.ac.uk

International Reviews in Physical Chemistry ISSN 0144–235X print/ISSN 1366–591X online © 2001 Taylor & Francis Ltd
http://www.tandf.co.uk/journals
DOI: 10.1080/01442350110062542

1. Introduction

The role of metal-containing molecules in chemistry is profound. In areas ranging from catalysis to biochemistry, atmospheric to interstellar chemistry, combustion to metal–organic vapour deposition, metal–ligand bonds (M—L bonds) are formed and broken. The M—L bond is therefore the bedrock of a whole swath of chemistry, and it is natural to seek a detailed understanding of its properties.

The most general means of probing the M—L bond is through detailed quantum–chemical calculations. Provided that the methodology is sophisticated enough, a virtually complete picture can be obtained. The equilibrium bond length, the bond dissociation energy, the bond force constant, the charge distribution and the effect of electronic excitation all can potentially be extracted from these calculations. Of course, *ab initio* calculations on metal-containing molecules are not easy. For a start, the electron count is usually quite high, making the calculations computationally intensive. The small separation of metal atomic orbitals often leads to many near-degeneracies for the molecular orbitals, meaning that highly correlated calculations are at least desirable, and often essential, further adding to the cost and the complexity. In the case of heavy metals, it is also necessary to allow for relativistic effects. All these factors taken together mean that it is rarely a trivial task to perform *ab initio* calculations on all but the simplest metal-containing molecules.

In order to calibrate any theoretical methodology, it is useful to tackle a number of simple test examples. Success in modelling these test species then leads to confidence in predictions for more sophisticated systems. In the case of metal-containing molecules, the simplest species consist of a single metal atom bound to a single attached molecule, the ligand. However, although simple from a theoretical point of view, the study of such molecules represents a major challenge to experimentalists. For most metals, attaching a single univalent ligand results in a highly reactive entity that has only a fleeting existence in the condensed phase.

A possible solution to this is to trap these molecules in rare-gas matrices, where the exceedingly low temperature and the surrounding inert host matrix slows the reaction rate to a negligible level. Matrix isolation techniques have played a major role in the study of reactive intermediates, including metal-containing species. However, there are a number of disadvantages with this approach. One is the rigid trapping site, which tends to quench any rotational motion, thus ruling out rotationally resolved spectroscopy. As serious, if not more so, is the perturbation of the molecule by the surrounding host lattice. The perturbation of vibrational states, at least low-lying vibrational states, is generally small [1]. Consequently, infrared (IR) and Raman spectra of matrix isolated molecules tend to compare

rather well with spectra of the same species recorded in the gas phase. In contrast, electronic spectra are usually severely perturbed, with exceedingly broad bands being the norm. In many cases it is difficult to extract any useful information from the spectra. This is unfortunate because electronic spectra, unlike IR and Raman spectra, can provide direct and valuable information on electronic structure.

The ideal environment to study reactive intermediates is in the gas phase. This review is concerned with the study of the electronic spectra of metal-containing molecules in the gas phase, and in particular the information that these spectra provide on electronic structure, equilibrium geometries, and vibrational and rotational properties. The focus is on *polyatomic* species containing main group metal atoms, specifically elements from groups 2 and 12 of the periodic table. All the molecules considered are free radicals. They have been chosen for several reasons, but principal among them is the ease with which they can be detected by laser-induced fluorescence (LIF) spectroscopy. Furthermore, we concentrate on work carried out since about 1990. Although a considerable amount of work on these molecules was carried out before this date, particularly for alkaline-earth-containing species, much of this work has already been reviewed elsewhere [2].

The choice of 1990 as the starting date for this review has the added significance that it was the first year in which supersonic jet cooling was employed in spectroscopic studies of alkaline-earth-containing free radicals. Using a Smalley-type laser ablation nozzle, Whitham *et al.* [3] showed that molecules such as CaOH, CaCCH and CaNC could be entrained within a supersonic jet and probed by LIF spectroscopy. Shortly thereafter Ellis *et al.* [4] showed that even larger molecules could survive the journey to the nozzle exit despite the violence of the laser ablation process. The first jet-cooled LIF spectrum of the calcium cyclopentadienyl radical CaC_5H_5 was reported. A new free radical containing a group 12 metal, CdC_5H_5, was also observed in the study by Ellis *et al.*

Since that early work there have been numerous reports of electronic spectra of polyatomic metal-containing species in supersonic jets. Important contributions have been made from a number of laboratories (see, for example Bernath *et al.* [5–7], Clouthier *et al.* [8–11], Merer *et al.* [12–15], Miller *et al.* [4, 16–26], Simard *et al.* [27–31] and Steimle *et al.* [32–46]). It would also be remiss of the present author to ignore work carried out without supersonic jets. Much work has been done in this category. Particularly noteworthy is the contribution of Ziurys *et al.*, who have employed millimetre-wave techniques to obtain pure rotational spectra of molecules produced in a Broida oven. Many intriguing species, such as alkali and alkaline earth monohydroxides, monoacetylides and monomethyls have been identified and characterized in their ground electronic states [47–75].

The remainder of this review is structured as follows. It begins with a brief description of experimental techniques that have been used to prepare metal-containing free radicals in the gas phase, with the emphasis on techniques employed in our laboratory. We then proceed to outline the electronic structure of alkaline-earth-containing free radicals, in order to set the scene for the description of spectroscopic results described subsequently. The review of spectroscopic work is biased towards, but by no means exclusively restricted to, work from our laboratory. This is organized into a number of sections. We begin with the lowest energy electronic transitions of alkaline-earth-containing free radicals, which have been extensively studied. Rather than review the complete field, molecules have been selected that both are interesting in their own right and, more importantly, will

underpin the discussion in later sections. Among these are the metal monohydroxides and monoacetylides. We then move on to consider new work on higher excited electronic states, including some intriguing new data on the alkaline earth isocyanides and cyanides. In the final section we consider group 12 species. Nominally similar to group 2 metals in that the valence orbital is a full *n*s orbital, the electronic spectra reveal important differences in the bonding in these molecules.

2. Experimental details

2.1. *Producing metal–ligand intermediates in the gas phase*

The most commonly used method for making free radicals in the gas phase involves fragmentation of a precursor molecule, normally by photolysis or by an electrical discharge. Unfortunately, these techniques have limited utility in the production of metal–ligand radicals (ML radicals), since suitable volatile precursors do not usually exist. As far as the work covered in this review is concerned, the only exceptions to this statement are the zinc monoalkyl free radicals, which can be obtained by ultraviolet (UV) photolysis or electrical discharge of the commercially available dialkyl zinc compounds [76]. All other ML radicals discussed in this review require an alternative strategy for production, and this involves reactions of metal atoms in the gas phase. To generate the metal atoms, either thermal evaporation or laser ablation is normally employed.

Most of the early work on ML radicals was carried out using a Broida-type oven source [77]. Metal atoms are produced by evaporation from a heated crucible and are entrained in a flow of inert carrier gas, usually Ar. At the exit of the crucible an oxidizing reagent is added. Reaction between the metal and the reagent usually proceeds briskly, often generating a chemiluminescent flame. For those reactions that are less facile, the rate can be dramatically enhanced by laser excitation of the metal atoms to populate metastable excited electronic states [78, 79]. The excess inert carrier gas aids in the cooling of the reaction mixture before it is probed spectroscopically. However, the temperature remains a serious disadvantage in many cases. At best a rotational temperature of about 400 K is attained with a Broida oven, and the vibrational temperature is often considerably higher on account of the much lower efficiency for the collisional cooling of vibrational degrees of freedom. This leads to highly congested spectra, which is especially troublesome when dealing with polyatomic molecules.

To eliminate this problem, supersonic cooling is necessary. Supersonic nozzles can be combined with hot oven evaporation upstream of the nozzle, but the technology is quite difficult to implement and these sources have not seen widespread use [80–83]. Far more common, and of more general utility, are pulsed laser ablation sources. These were developed almost simultaneously and independently by Smalley *et al*. [84] and Bondybey *et al*. [85] in the early 1980s. The concept is simple. With a sufficiently high-intensity laser, as is frequently achieved by focusing the beam from any reasonably high-energy commercial pulsed laser, almost any metal (or indeed any other solid target) can be ablated. In the Smalley-type source, ablation takes place prior to expansion into vacuum in the presence of flowing inert carrier gas. One or more reagents can be seeded into the carrier gas to bring about reaction with the metal atoms produced by ablation. The mixture is then expanded into a vacuum chamber to form a supersonic jet. The laser ablation nozzle employed in our laboratory is shown in figure 1. Using this source, we can readily produce metal-

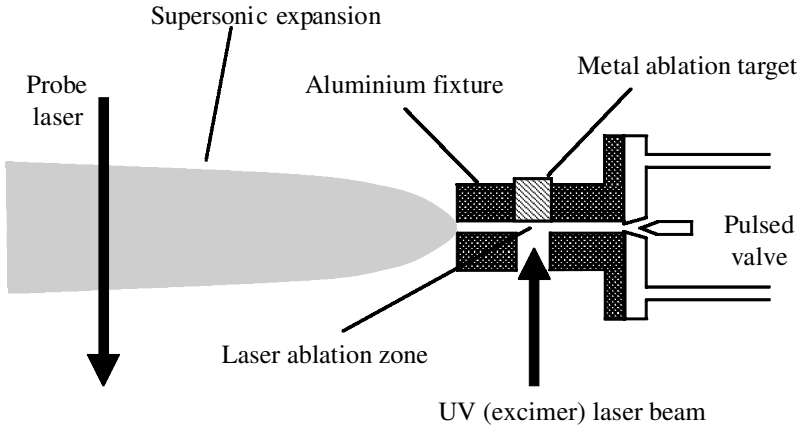

Figure 1. Diagram illustrating the laser ablation nozzle used in our laboratory. Further details concerning this source have been given by Beardah and Ellis [86].

containing molecules with rotational temperatures below 15 K, and vibrational temperatures well below room temperature are also frequently obtained.

It is important to recognize that laser ablation is rarely a clean source of a particular species. A multitude of processes can take place in the laser ablation region. In addition to metal atoms, which can be formed in both their ground state and their excited electronic states, metal clusters and metal ions can also be generated. The bombardment by intense laser radiation, and the subsequent production of light, heat and a whole host of charged particles within the ablation plasma, can lead to extensive fragmentation of molecular precursors. The lack of species discrimination is illustrated by the LIF spectrum shown in figure 2. This spectrum was obtained by laser ablation of a Ca target in the presence of benzene in excess Ar. Strong fluorescence signals from several Ca-containing free radicals are observed, and of course these only represent a subset of the full array of species that may have been produced in the nozzle source.

Finally, we note that that there is an alternative to the laser ablation method for generating supersonically cooled metal-containing free radicals by metal atom reactions. This alternative uses an electrical discharge to generate metal atoms by sputtering from an electrode surface. A number of research groups, including our own, have combined the sputtering phenomenon with supersonic nozzles. In our own case, a novel dual-channel nozzle was developed to produce organometallic molecules [87]. This nozzle, shown schematically in figure 3, is designed to separate the reactive precursor from the region where metal atoms are produced. This proved to be essential because, if a single channel was used, rapid decomposition of the organic precursors was found to occur in the discharge. This lead to the deposition of C deposits on the surface of the sputtering electrode (the cathode) and quickly terminated the metal sputtering. In the dual-channel nozzle, the two gas streams, one containing metal atoms plus inert carrier gas, and the other containing a molecular reagent plus inert carrier gas, are combined just prior to expansion. The turbulence at the junction of the channels ensures efficient mixing as the gas begins to expand into vacuum. The principal advantage of the dual-channel discharge is its low cost relative to laser ablation sources. The main disadvantage is that sputtering

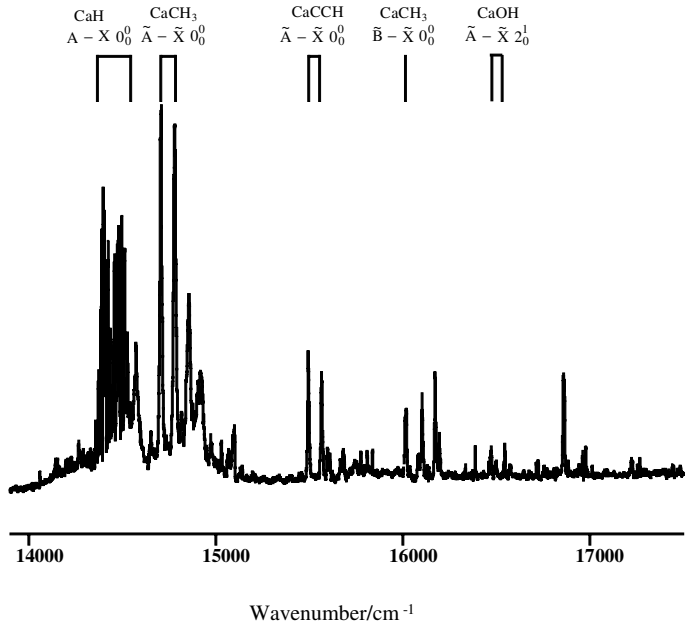

Figure 2. Laser excitation spectrum obtained following laser ablation of Ca in the presence of benzene (1%) seeded in Ar.

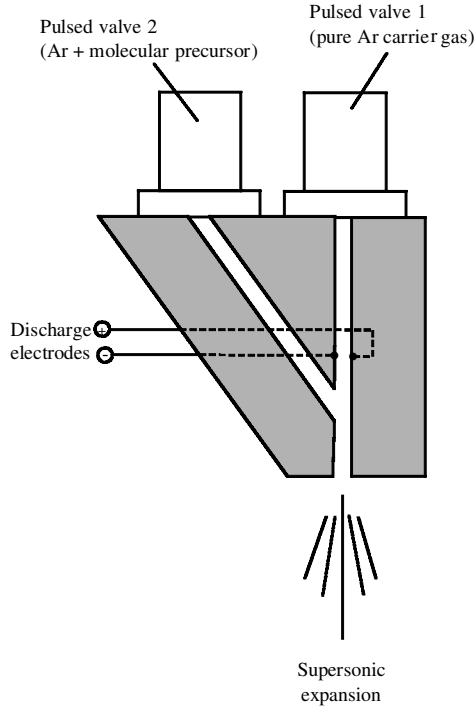

Figure 3. Schematic view of a dual-channel discharge nozzle. A full description of the nozzle construction, including the actual design of the discharge electrodes (more complex than indicated here), has been given by Bezant *et al.* [87].

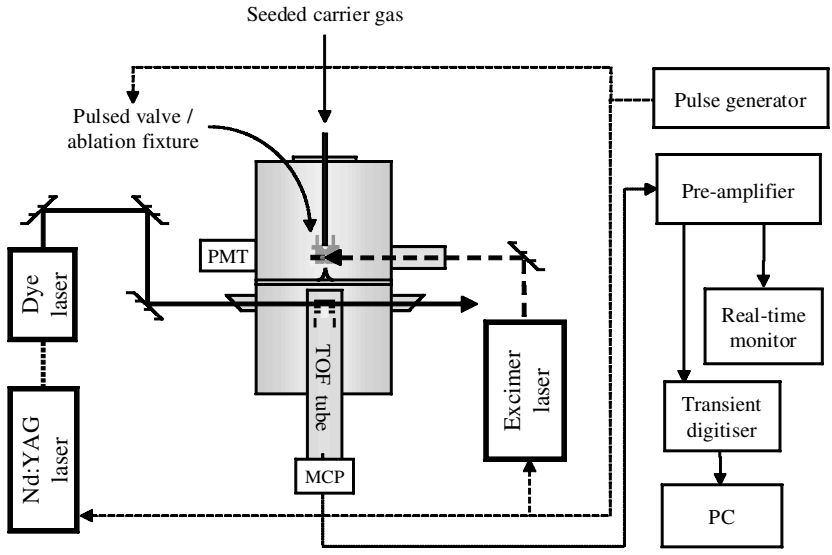

Figure 4. Block diagram showing the overall experimental arrangement: PMT, photomultiplier tube; MCP, microchannel plate detector; Nd:YAG, neodymium-doped yttrium aluminium garnet; PC, personal computer. The tunable dye laser beam is shown entering the ion source of a time-of-flight mass spectrometer, the arrangement used for REMPI experiments. For LIF spectra the dye laser beam crosses the supersonic jet *upstream* of the skimmer.

efficiencies can vary strongly from one metal to another, and so this method is less general than laser ablation. Sputtering is further inhibited by the formation of oxide layers on the metal surface. Consequently, while the dual-channel nozzle has been used to produce some of the Zn- and Cd-containing free radicals described in section 7.1, it is unsuitable for the generation of alkaline-earth-containing radicals.

2.2. *Spectroscopic techniques*

The majority of electronic spectra shown and discussed in this review were recorded using LIF spectroscopy. This standard technique is ideally suited to the strongly fluorescing molecules described here. In our laboratory, resonance-enhanced multiphoton ionization (REMPI) spectroscopy is sometimes used as an alternative when there is ambiguity about the spectral carrier. With REMPI spectroscopy the mass of the absorbing molecule (or some fragment of it) can be determined by mass-selective detection of the ions formed. The overall apparatus employed in our laboratory is shown schematically in figure 4. Further details can be found elsewhere [88, 89].

3. A simple orbital model for the electronic structure of metal–ligand molecules

In this section we outline the expected electronic structure of alkaline-earth-containing ML radicals. The electronic structures of group-12-metal-containing radicals is discussed later when the spectra of these molecules are considered.

Alkaline earth atoms have relatively low ionization energies and therefore tend to form compounds dominated by ionic bonding. The normal oxidation state of the alkaline earth atoms is + 2, corresponding to the transfer of both valence s electrons

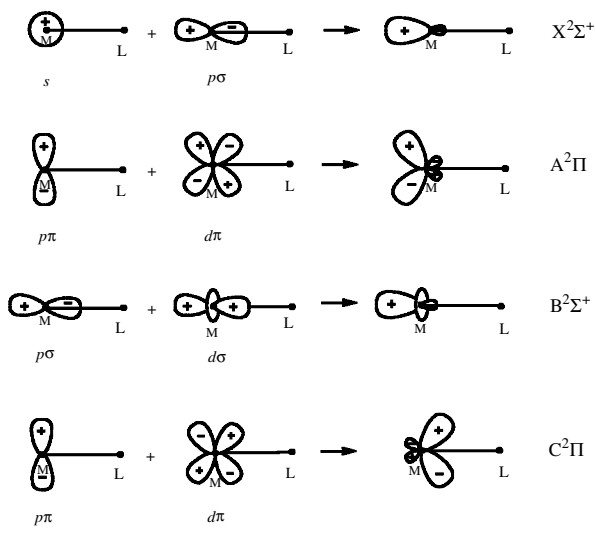

Figure 5. Diagram illustrating the effect of mixing different s, p and d orbitals to produce a polarized unpaired electron distribution on the metal atom. The orbital compositions implied for the electronic states shown in this figure are only approximate.

to one or more ligands of greater electronegativity. However, when there is only one ligand, as is the case for the molecules covered in this review, both +1 and +2 oxidation states are possible. For ligands such as OH and CN, only singly charged anions can be formed and therefore in MOH or MCN the metal will be forced to adopt an oxidation state of +1.

Nominally, the unpaired electron remaining on the metal atom has s character in the electronic ground state. However, in practice, electron–electron repulsion between the unpaired electron and the electron cloud of the anion will lead to redistribution of the former to minimize the repulsion. This can be achieved through mixing of the *n*sσ orbital with the *n*pσ orbital on the metal atom, as shown in figure 5. The resulting polarization of the unpaired electron density on the opposite side of the metal from the ligand was first suggested by Knight *et al.* [90] in their interpretation of hyperfine coupling in electron spin resonance (ESR) spectra of alkaline earth monohalides. *Ab initio* calculations, which are discussed in more detail in the next section, have subsequently confirmed the qualitative validity of this model (see, for example, Bundgen *et al.* [91]).

The presence of an unpaired electron results in relatively low-lying electronic transitions, making these molecules particularly favourable for observation by laser electronic spectroscopy. These low-lying transitions are strongly metal centred. The alternative possibility, charge-transfer excitations in which electron density is shifted from the ligand towards the metal, will tend to have a much higher energy. Consequently, in order to understand the known electronic spectroscopy of these molecules, it is acceptable to construct a molecular orbital diagram in which the metal atomic orbitals play the dominant role. Of course the energies of these orbitals will be strongly affected by the presence of the ligand but, provided that the unpaired electron density resides largely on the opposite side of the metal from the anion, the precise ligand identity will be of secondary importance. As a result, the low-lying

electronic transitions for a multitude of ML radicals should occur at roughly similar energies and this is indeed observed in practice.

This simple orbital model is shown in figure 6. Ca has been chosen as the metal for this illustration, but it is straightforward to adapt this picture for the other alkaline earth elements and a variety of ligands. Two scenarios are represented in figure 6. If the molecule is linear, the pattern of electronic states shown in the central column results. The excited states are shown as possessing mainly 4p and 3d character. This is obviously a simplified description, since it is possible for both higher- and lower-energy atomic orbitals of the correct symmetry to contribute, but it is nevertheless approximately correct.

The ordering of the three lowest excited electronic states is easily rationalized by considering the orbital hybridizations shown in figure 5. This figure shows the required combination of metal atomic orbitals to produce a polarization away from

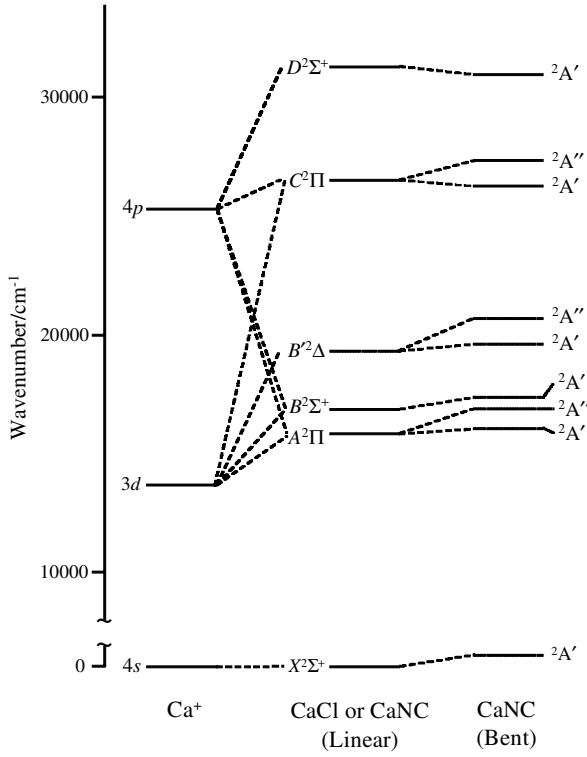

Figure 6. Energy level diagram showing the correlation of electronic states of CaL radicals with the orbitals of Ca^+. For CaCl, note that the $B'^2\Delta$ state has not been observed experimentally, and theoretical predictions are divided as to whether it lies above or below the $B^2\Sigma^+$ state [92, 93]. For the nonlinear molecule, the $^2A'$ state is always shown below the $^2A''$ state for those $^2A'$–$^2A''$ pairs resulting from the loss of orbital degeneracy. Although there is no guarantee that this ordering applies in every case, a combination of spectroscopic [40, 194] and theoretical [95] evidence does at least indicate that it applies for CaSH, a molecule which is known to be bent. The lower energy of the $^2A'$ state for the $^2A'$–$^2A''$ pairs in CaSH can be rationalized by noting that a σ bonding interaction is possible between the orbital containing the unpaired electron on Ca with one of the lone pair orbitals on the S for the $^2A'$ state. Symmetry prevents any such stabilization of the $^2A''$ state.

the ligand. For both Σ and Π electronic states, strong polarization can be achieved by the mixing of 4p and 3d orbitals. The lowest in energy of these two states should be the Π state since there is no electron density along the internuclear axis, thus minimizing the electron–electron repulsion between the metal and ligand. In contrast the lowest Δ state (not shown in figure 5) requires the addition of 4fδ character to the 3dδ orbital to achieve the desired polarization. Since the former orbital is generally much higher in energy than the latter, particularly for the lighter alkaline earths, polarization away from the ligand is far less effective for the lowest Δ state. Consequently, on the basis of these simple qualitative arguments, we would predict the three lowest-lying excited electronic states to have the energy order $^2\Pi < {}^2\Sigma^+ < {}^2\Delta$. The limitations of these arguments are worth emphasizing, since exceptions to this ordering are known (an example is discussed later).

The right-hand column of figure 6 shows the effect of lowering the symmetry of the molecule. For the C_s point group, all orbital degeneracies are removed. However, the splitting of states due to the loss of degeneracy would not be expected to be large, since the ligand is distant from the bulk of the unpaired electron density. As a result, the ordering and character of the states can be viewed largely in terms of the linear molecule picture, with the lowering of symmetry providing a modest perturbation. Examples demonstrating the validity of this description will be given later.

4. Beyond the qualitative orbital model: quantitative predictions

4.1. *Classical electrostatic and ligand field models*

More sophisticated and quantitative models of the electronic structure of ML radicals have been developed. Classical ionic models based upon the Rittner description of polarizable ions have been applied to the alkaline earth monohalides. In the original Rittner [96] model the effect of mutual ion polarization on the electrostatic binding energy is treated by expanding the ion polarizabilities in power series in $1/r$. The expansion is then truncated such that the highest-order interaction term is the induced dipole–induced dipole term. This is perfectly adequate for the alkali halides, but higher-order multipole interactions are important for the group 2 halides on account of the much larger polarizabilities of the alkaline earth atoms. If these are not taken into account, then the calculations do not even yield permanent electric dipole moments with the correct sign! Consequently, the Rittner model must be extended in order to deal with alkaline-earth-containing species.

Klynning and Martin [97, 98] used a modified version of the Rittner model, the Rittner–Lawley model, to calculate the properties of CaCl. They found that the experimentally determined ground state potential energy curve could be fitted rather well to the Rittner–Lawley potential. However, subsequent work using this model yielded a ground-state dipole moment in very poor agreement with experiment. A more sophisticated electrostatic model was subsequently developed by Torring *et al.*, which takes into account the large shift in the centre of charge in the metal ion resulting from polarization by the ligand. This gave good agreement with experiment for the dissociation energies and dipole moments of the ground electronic states of the alkaline earth monohalides [99]. This model was subsequently extended to the low-lying excited electronic states, and again reasonable agreement with experimental data was obtained where such data were available [92]. The Torring *et al.* approach was subsequently applied to the alkaline earth monohydroxides by Mestdagh and Visticot [100]. These workers extended the Torring *et al.* model by

allowing for the shift in the centre of charge on the ligand as well as the metal. Again, reasonable agreement with experimental data was obtained for the ground and low-lying excited electronic states.

A serious problem with classical electrostatic models is the need for several adjustable parameters. Rice *et al.* [93] have presented an alternative model of the electronic structure of the alkaline earth monohalides based on a ligand field description. In contrast with the Rittner model and its variants, the ligand field approach incorporates a quantum-mechanical treatment through the use of wave-functions for the free metal cations. The electrostatic field created by the polarizable halide ion causes mixing of the cation orbitals and this mixing is elucidated by using the free ion orbitals as basis functions for a perturbation theory treatment. With this approach Rice *et al.* were able to calculate a variety of properties including electronic state energies, permanent electric dipole moments, electronic transition dipole moments and spin–orbit splittings. The agreement with experiment was mostly good. Allouche and Aubert-Frecon [101] have extended the ligand field model of Rice *et al.* to the alkaline earth monohydroxides, but so far this is the only application to polyatomic alkaline-earth-containin g molecules.

The general picture that emerges from the classical electrostatic and ligand field calculations confirms and extends the description given in the previous section. For example, it is now clear that the $X\,^2\Sigma^+$ state is predominantly *n*s in character but with a substantial admixture of *n*pσ character to polarize the unpaired electron density on the opposite side of the metal from the ligand. The $A\,^2\Pi$ state is predominantly *n*pπ in character in most of the ML molecules but there is also a sizeable, and in the case of the Ba-containing species a dominant, contribution from the $(n-1)$dπ orbitals. As higher states are accessed, the contribution of the *n*p orbital lessens. This is useful information in interpreting electronic spectra of these and related molecules, as are the dipole moments calculated for the ground state and low-lying excited electronic states.

Overall, both the Rittner-based models and the ligand field description have proved useful in providing insight into the properties of these molecules. However, neither is easily applied to polyatomic species. Furthermore, improvements in computer power over the past decade or so and the more widespread availability of such facilities mean that *ab initio* calculations can now take the place of these somewhat simplistic models. It is to the former that we now turn.

4.2. *Ab initio calculations*

There have been many *ab initio* calculations on ML radicals. We start by considering work on the ground electronic states of these molecules. Rather than attempting a comprehensive review, the focus here is on polyatomics, since these are the primary interest in this article. Some of the earliest and most exhaustive *ab initio* calculations on alkaline-earth-containin g free radicals were reported by Bauschlicher *et al.* As well as dealing with the monohalides [102, 103], these workers also investigated MOH and MCN radicals using the CISD method (configuration interaction with single and double excitations). For L = CN, both the cyanide and the isocyanide structures were considered and it was firmly established that MNC is substantially lower in energy than MCN for all the alkaline earths [104]. As expected, these molecules are highly ionic and it is this that favours adoption of a linear structure at equilibrium.

Several *ab initio* calculations on the monohydroxides have been reported. The OH ligand is less electronegative than CN (the respective vertical electron affinities are 1.82 eV [105] and 3.82 eV [106]), and therefore greater covalent character might be expected in the M—OH bonding, particularly for the lighter metals Be and Mg. If substantial covalent character occurs, the lone pairs on O will force the molecule to bend. Bauschlicher *et al.* [107] carried out CISD calculations on MOH where M = Be → Ba. CaOH, SrOH and BaOH were found to be linear, a finding confirmed by experimental observations (see later) and strongly supporting the notion that the M—OH bonding in these molecules is predominantly ionic. MgOH was also found to be linear, but with a very flat bending potential, suggesting that covalent character is beginning to play an important role. Unsurprisingly, given the result for MgOH, BeOH was calculated to be bent at equilibrium, with an estimated barrier to linearity of 60 cm^{-1}. Other theoretical work [108–111] has supported these general conclusions.

Ab initio calculations have also been used to search for other stable isomers of MOH. Internal rotation of OH to give MHO does not yield a minimum on the ground-state potential energy surface. However, the linear HMO isomers do appear to give true minima which, for Be, Mg and Ca, all lie approximately 2.6 eV above that of MOH [112, 113]. No experimental observations of the metastable HMO isomers have been reported to date.

Published *ab initio* work on larger ML radicals is relatively sparse. Tyerman *et al.* [114] reported self-consistent field and second-order Møller–Plesset calculations on the ground electronic states of $BeCH_3$, $MgCH_3$ and $CaCH_3$. Woon [115] has carried out high quality *ab initio* calculations on MgCCH (together with MgCN and MgNC) to establish spectroscopic parameters which might serve as a useful guide for identifying this molecule in space. However, by far the most comprehensive survey of ML radicals has appeared in two recently published papers by Chan and Hamilton [116, 117]. These workers employed the B3LYP density functional method combined with modest sized basis sets (double zeta + polarization) to calculate the equilibrium structures and harmonic vibrational frequencies of a wide range of ML radicals, where L varied from halide atoms through to relatively large ligands such as acetate (CH_3COO) and cyclopentadienyl (C_5H_5).

Only a handful of publications have dealt with *ab initio* calculations on excited electronic states. Electronic excited states are notoriously much more difficult to deal with than electronic ground states, and attempts to achieve quantitative accuracy often require recourse to sophisticated multireference calculations. Several studies have focused on diatomics [115–125], but some work on polyatomics has also been carried out. In an effort to explain the lack of Stark broadening in the rotationally resolved $\tilde{A}\,^2\Pi$–$\tilde{X}\,^2\Sigma^+$ electronic spectrum of CaOH, Bauschlicher *et al.* [126] used *ab initio* calculations to determine the dipole moments in the $\tilde{X}$, $\tilde{A}$ and $\tilde{B}$ states. Small dipole moments (less than 1 D) were observed for all three states despite their highly ionic character. Based on the discussion in section 3, this is easily explained by the strong polarization of the unpaired electron density on Ca^+. The predicted magnitudes of the dipole moments were shown to be in good agreement with the upper limit for the $\tilde{A}\,^2\Pi$ state estimated from the absence of observable Stark broadening [126]. More recent theoretical work on the excited electronic states of alkaline earth monohydroxides has dealt with BeOH and MgOH [109]. Both of these molecules are predicted to possess bent first excited electronic states, in contrast with CaOH, and in the case of MgOH this ties in nicely with experimental findings.

Other reports of *ab initio* calculations on excited electronic states of polyatomic ML radicals include studies of the $\tilde{A}$-$\tilde{X}$ electronic transitions of $MgCH_3$ and MgCCH by Woon [127, 128], as well as an investigation of the ground state and first two excited electronic states of the CaNC–CaCN system by Nanbu *et al.* [129].

A rather different approach to the calculation of electronic excitation energies in ML radicals has been adopted by Ortiz. This employs electron propagator methodology to determine the vertical electron affinities of the ML^+ cation. The electron affinities are calculated directly (by a means which is, in a sense, analogous to Koopmans' theorem) rather than as energy differences between two states. Differences between these electron affinities then provide the excitation energies of the neutral molecule. Furthermore, information can be deduced on how the electronic structure of the neutral differs from the cation. Ortiz has applied this approach to a range of CaL free radicals including CaF, CaOH, $CaNH_2$, $CaCH_3$ [130], CaSH [95], $CaBH_4$ [131], CaC_5H_5 [132], and CaNC–CaCN [133]. In general the agreement with experimental electronic excitation energies is quite good, typically better than 0.1 eV.

5. Experimental studies of low-lying electronic states of alkaline-earth-containing radicals: the ligand as spectator

5.1. *Introduction*

In this review we identify the low-lying electronic states as the $\tilde{X}\,^2\Sigma^+$, $\tilde{A}\,^2\Pi$, $\tilde{B}\,^2\Sigma^+$ and $\tilde{B}'\,^2\Delta$ states, or their equivalents in nonlinear molecules. Transitions from the ground electronic state to the $\tilde{A}\,^2\Pi$ and $\tilde{B}\,^2\Sigma^+$ states are generally very strong for all alkaline-earth-containing free radicals and fall within convenient regions of the spectrum for laser excitation. Furthermore, the fluorescence quantum yields are often very high, making them amenable to study by LIF spectroscopy. The $\tilde{B}'\,^2\Delta$ states are more difficult to study because the $\tilde{B}'\,^2\Delta$-$\tilde{X}\,^2\Sigma^+$ transition is nominally forbidden by the $\Delta\Lambda = 0, \pm 1$ selection rule. Nevertheless, this transition has been observed for a number of molecules and examples will be discussed later.

Many aspects of the spectroscopy of the low-lying electronic transitions of alkaline-earth-containing free radicals have been reviewed elsewhere [2]. Consequently, we focus here on a select group of specific examples. The purpose of this is twofold:

(i) to review some new developments, particularly those resulting from application of supersonic jets, and
(ii) to provide important background information necessary for appreciating studies of higher electronic states described in section 6.

5.2. *Some specific examples*

5.2.1. *MCCH*

We start with a discussion of the alkaline earth monoacetylides. These are among the simplest of the alkaline earth containing free radicals, and so an account of their electronic spectra and properties sets the scene for more complex species.

Of the two lightest group 2 monoacetylides, BeCCH and MgCCH, very little work has been done on the former. In fact the only spectroscopic observation of BeCCH reported to date has been a matrix isolation IR study by Thompson and Andrews [134]. These workers made BeCCH by laser ablation of Be metal in the presence of acetylene. This was a somewhat courageous experiment given the known

toxicity of Be, and indeed concerns over its high toxicity may explain why no other spectroscopic work has been carried out on BeCCH. Thompson and Andrews combined data from the isotope shifts of IR bands with density functional calculations to assign three of the five vibrational fundamentals, the Be—C and C≡C stretches and the CCH bend.

The first spectroscopic observation of MgCCH was made by Anderson and Ziurys [135]. Using millimetre wave direct absorption spectroscopy, 17 pure rotational transitions of this molecule were recorded. The motivation for this work stemmed from an earlier observation of both MgNC and MgCN in the outer envelope of a C-rich star, IRC + 0216 [136, 137]. Since Mg is the most abundant metal in the universe, and given that both HCCH and CCH are both relatively abundant in IRC + 10216, the detection of other Mg-bearing species, including MgCCH, must be a distinct possibility. The pure rotational spectra were consistent with a linear molecule with a $^2\Sigma^+$ ground electronic state, although small deviations from linearity could not be ruled out.

Subsequent work has supported the view that MgCCH is linear. Woon [115] carried out CCSD(T) calculations with several basis sets, including the large quadruple zeta cc-pVQZ basis. In all cases the molecule was found to be linear at equilibrium.

The first electronic spectrum of MgCCH was recorded in our laboratory using LIF spectroscopy of a jet-cooled sample [138]. The low-resolution laser excitation spectrum, shown in figure 7, is relatively sparse and very easy to assign. A short

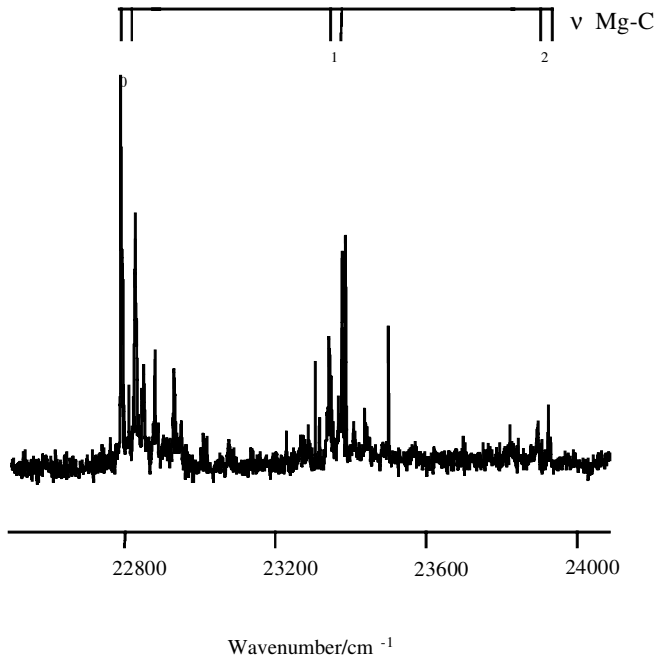

Figure 7. Laser excitation spectrum of the $\tilde{A}\,^2\Pi$-$\tilde{X}\,^2\Sigma^+$ system of MgCCH. The doublet seen for each vibrational component, located by the vertical bars above the spectrum, is due to spin–orbit coupling in the $\tilde{A}\,^2\Pi$ state. (Reproduced from [138] with permission from Elsevier Science.)

progression in a single vibrational mode, the Mg—C stretch, dominates the spectrum. A short progression is consistent with the expectation that the low-lying electronic transitions of ML radicals are metal localized (non-bonding → non-bonding). Within each vibrational component there is additional structure due to weak sequence bands and spin–orbit splitting. By analogy with the electronic states of CaL radicals shown in figure 6, the first excited electronic state of MgCCH is expected to be a $^2\Pi$ state. The observation of a spin–orbit doubling of about 35 cm^{-1} within each vibrational component is therefore strong evidence that the $\tilde{A}\,^2\Pi$-$\tilde{X}\,^2\Sigma^+$ transition is being observed, as well as proving that MgCCH is also linear in its first excited electronic state. This assignment has been confirmed by a subsequent *ab initio* study of the $\tilde{A}\,^2\Pi$-$\tilde{X}\,^2\Sigma^+$ transition of MgCCH by Woon [128].

There is now a considerable body of information on the $\tilde{X}$ and $\tilde{A}$ states of MgCCH. Laser-excited emission spectra of MgCCH have been recorded in our laboratory which, in combination with data from matrix isolation IR work [134], has allowed four of the five vibrational fundamentals to be established [139]. Millimetre-wave spectra of MgCCH in the $\nu = 1$ MgCC bending vibrational level have also been recorded [140]. The picture that emerges from all these data is of a fairly rigid linear molecule. A substantial degree of covalent character is expected in the Mg—C bond, but it seems that this is insufficient to produce any significant tendency towards a bent structure. It is worth noting, however, that CCH may be a rather special ligand in this regard since the acetylinic π system may enhance the preference for linearity through its interactions with π orbitals on the metal. In the case of the $\tilde{X}\,^2\Sigma^+$ state, this may take the form of back bonding into vacant π orbitals on the Mg. In the $\tilde{A}\,^2\Pi$ state the partly filled π orbital on the metal may partake in some covalent bonding with the acetylinic π system. Tentative support for this suggestion comes from the observation of an increase in both the Mg—C stretching frequency and the rotational constant on $\tilde{A}$ $\tilde{X}$ excitation [138], although the increases are modest.

Continuing down group 2, the next two monoacetylides, CaCCH and SrCCH, were in fact the first alkaline earth monoacetylides to be observed experimentally. The initial detection of these molecules was made by Bopegedera *et al.* [141], who combined a Broida oven source with LIF spectroscopy to record the $\tilde{A}\,^2\Pi$-$\tilde{X}\,^2\Sigma^+$ spectrum. The very low resolution (about 50 cm^{-1}), caused by rotational broadening due to the high sample temperature, limited the information that could be obtained. Nevertheless, it proved possible to extract some ground electronic state vibrational frequencies, as well as the spin–orbit coupling constants in the $\tilde{A}\,^2\Pi$ state. The $\tilde{A}$ state spin–orbit couplings for CaCCH (73 cm^{-1}) and SrCCH (275 cm^{-1}) are much larger than for MgCCH, in line with the increase in atomic spin–orbit coupling constants on the respective metal atoms. Surprisingly, given the observation of $\tilde{B}$-$\tilde{X}$ transitions for many other ML radicals, Bopegedera *et al.* could find no trace of the $\tilde{B}\,^2\Sigma^+$-$X\,^2\Sigma^+$ transition in the LIF spectra of CaCCH or SrCCH. The same result was also found by our group for MgCCH, suggesting perhaps that in all three molecules the $\tilde{B}\,^2\Sigma^+$ state is predissociated.

Subsequent work has provided a glut of detailed information on CaCCH in particular. Rotationally resolved spectra of the $\tilde{A}$-$\tilde{X}$ transition have been analysed by several groups to obtain rotational constants in both electronic states [3, 142, 143]. The most comprehensive, and most precise, work has been that by Li and Coxon [143], who used a narrow-linewidth continuous-wave dye laser system to record 440 lines in the LIF spectrum of the $\tilde{A}$-$\tilde{X}$ 0_0^0 transition. Marr *et al.* [38] have

carried out an optical Stark measurement of the $\tilde{A}$-$\tilde{X}$ system of CaCCH under molecular-beam conditions in order to determine the dipole moments of the $\tilde{X}\,^2\Sigma^+$ and $\tilde{A}\,^2\Pi$ states. The relatively small values obtained, 3.01 ± 0.01 and 2.41 ± 0.02 D respectively, are readily explained in terms of a highly ionic model for the Ca—C bonding when the polarizabilities of the Ca^+ and CCH^- ions are taken into account.

Li and Coxon [144–147] have performed several high-resolution studies of CaCCH in order to obtain detailed information on the bending vibrational levels in the $\tilde{X}\,^2\Sigma^+$ and $\tilde{A}\,^2\Pi$ states. As part of this work the Renner–Teller effect in the $\tilde{A}\,^2\Pi$ state was characterized and the Renner parameters for both the CaCC and the CCH bending vibrations were found to be very small [145, 147]. This is explained by the localization of the π orbital on the metal and its polarization away from the ligand. Weak coupling of the orbital and vibrational angular momenta is therefore a result of the physical remoteness of the π electron from the CCH unit.

To close the discussion of CaCCH and SrCCH, it is interesting to note that nominally forbidden transitions have recently been observed for both molecules. Elhanine *et al.* [148] reported the $\tilde{C}\,^2\Delta$-$\tilde{X}\,^2\Sigma^+$ LIF spectrum of jet-cooled CaCCH. Although forbidden electronically by the $\Delta\Lambda = 0, \pm 1$ selection rule, this transition is vibronically allowed through coupling between the vibrational angular momentum of the CaCC bending mode and the orbital angular momentum of the electron. The $\tilde{C}\,^2\Delta$ state identified by Elhanine *et al.* is the equivalent of the $\tilde{B}'\,^2\Delta$ state shown in figure 6. We have recently identified the analogous states for SrCCH and SrCCD. The LIF excitation spectra are shown in figure 8 [149]. In SrCCH, it is plausible that spin–orbit coupling rather than vibronic coupling could overcome the $\Delta\Lambda = 0, \pm 1$ selection rule. However, if spin–orbit coupling was responsible, the Ω quantum number should be conserved, which would selectively enhance only the lower spin–orbit component in each doublet. This is not observed, and so it appears that, like

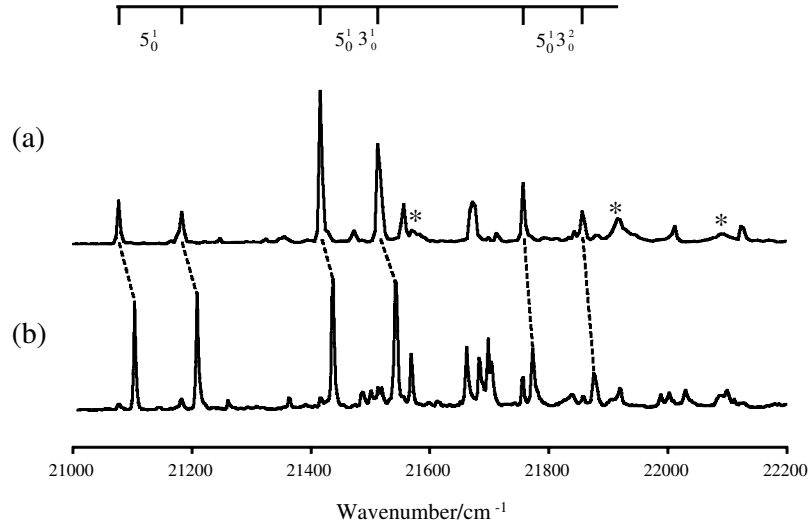

Figure 8. Laser excitation scans showing the vibronically induced $\tilde{B}'\,^2\Delta$-$\tilde{X}\,^2\Sigma^+$ spectra of (a) SrCCH and (b) SrCCD. Modes ν_3 and ν_5 are the Sr—C stretching and SrCC bending modes respectively, with ν_5 being responsible for the vibronic coupling. (Reproduced from [149] with the permission of Academic Press.)

CaCCH, observation of the lowest $^2\Delta$-$^2\Sigma^+$ transition is the result of vibronic coupling in the excited electronic state.

Finally, we note that no spectroscopic data of any type have so far been reported for BaCCH.

5.2.2. *MOH*

The monohydroxides have been the most extensively studied group of monoligated alkaline earth containing free radicals. The two lightest species, BeOH and MgOH, have received the least attention from experimentalists. Indeed for BeOH there has been only one reported spectroscopic study of this molecule (and its isotopomer BeOD). In this work, Anticjovanovic *et al.* [150] employed an arc discharge across Be electrodes in the presence of H_2O (D_2O) vapour to obtain an emission spectrum. No independent confirmation of these findings has been reported, so the assignment to BeOH must be viewed with some caution. Nevertheless, *ab initio* calculations [109] predict the $\tilde{\mathbf{A}}$-$\tilde{\mathbf{X}}$ transition to be close to the band positions (300–330 nm) observed by Anticjovanovic *et al.*, thus lending some support to the BeOH assignment. As mentioned in section 4.2, BeOH is calculated to be bent in its ground electronic state, a consequence of covalent character in the Be—O bond, although the bending potential is very flat. The molecule was also predicted to be bent in its first two excited electronic states. These excited states have $^2A'$ and $^2A''$ symmetry, with the former lying lower, and they correlate with the $\tilde{A}\,^2\Pi$ state that would be formed were BeOH linear. New spectroscopic work on BeOH would clearly be welcome, although as noted earlier the high toxicity of Be is an obstacle.

Ni [151] was the first to suggest that MgOH was bent in its first excited electronic state. Using LIF spectroscopy, this worker identified the $\tilde{\mathbf{A}}$-$\tilde{\mathbf{X}}$ system of MgOH. Vibrationally resolved dispersed fluorescence spectra revealed the shape of the ground-state bending potential function, and it was shown that a linear structure with a very flat (strongly quartic) bending potential was consistent with the experimental data. Subsequent work has confirmed that view [68]. A vibrational analysis of the excitation spectrum led to the conclusion that the first excited electronic state is a $^2A'$ state and is the lower member of a Renner–Teller pair correlating with a $^2\Pi$ state. This is similar to BeOH. The barrier to linearity in the $\tilde{A}\,^2A'$ state of MgOH was estimated to be 1970 cm^{-1}, which is in good agreement with recent *ab initio* calculations by Theodorakopoulos *et al.* [109], who obtained a barrier height of 2216 cm^{-1}. The calculations also found that the $\tilde{\mathbf{A}}\,^2A'$ and $\tilde{\mathbf{B}}\,^2A''$ states share similar equilibrium bond angles, 115° and 120° respectively. However, no spectra have so far been reported for the $\tilde{\mathbf{B}}$-$\tilde{\mathbf{X}}$ transition of MgOH.

CaOH and SrOH have been the subjects of many detailed spectroscopic investigations [43, 44, 46, 126, 152–165]. The conclusion that emerges for both molecules is of a strongly ionic M—O bond in the ground state and first two excited electronic states. Both low- and high-resolution LIF spectra have shown that these molecules are linear in their ground state and first two excited electronic states, as expected for ionic species. Furthermore, calculations using the classical electrostatic polarization and ligand field models discussed in section 4.1, as well as *ab initio* calculations, all support the strongly ionic model. Thus their electronic structure is analogous to that of CaCl shown in figure 6. In fact, an abundance of information on CaOH and SrOH has now been amassed from high-resolution LIF studies. This has included very precise rotational constants for both MOH and MOD, spin–

Table 1. Experimental[a] and theoretical[b] dipole moments of CaOH and SrOH.

Electronic state	Dipole moment (D)			
	CaOH		SrOH	
$\tilde{X}\,^2\Sigma^+$	1.465 ± 0.061	(experiment)	1.900 ± 0.014	(experiment)
	1.2	(EPM)	1.8	(EPM)
	1.465	(LF)	1.900	(LF)
	0.98	(*ab initio*)		
$\tilde{A}\,^2\Pi$[c]	0.836 ± 0.032	(experiment)	0.590 ± 0.045	(experiment)
	0.4	(EPM)	0.2	(EPM)
	1.6	(LF)	1.4	(LF)
	0.49	(*ab initio*)		
$\tilde{B}\,^2\Sigma^+$	0.744 ± 0.084	(experiment)	0.396 ± 0.061	(experiment)
	−0.6	(EPM)	−1.0	(EPM)
	2.2	(LF)	1.6	(LF)
	0.11	(*ab initio*)		

[a] Experimental values from optical Stark measurements by Steimle *et al.* [46].
[b] EPM, classical electrostatic polarization model [100]; LF, ligand field model [101]; the *ab initio* results were from [126].
[c] Experimental data shown are for the $^2\Pi_{1/2}$ spin–orbit component. For the $^2\Pi_{3/2}$ state the measured dipole moments were 0.766 ± 0.024 and 0.424 ± 0.005 D for CaOH and SrOH respectively [46].

rotation and spin–orbit parameters, and a detailed characterization of the Renner–Teller effect in the $\tilde{A}\,^2\Pi$ state [43, 44, 152–161].

The permanent electric dipole moments of CaOH and SrOH in their $\tilde{X}\,^2\Sigma^+$, $\tilde{A}\,^2\Pi$ and $\tilde{B}\,^2\Sigma^+$ states have been determined by Steimle *et al.* [46] using optical Stark spectroscopy. The values obtained are summarized in table 1, where they are compared with theoretical predictions from various sources. Theory and experiment agree that the dipole moments are relatively small in all the low-lying electronic states. As mentioned earlier, this can be accounted for within a highly ionic bonding model by the large polarizability of the M^+ ion and, to a lesser extent, that of OH^-, which serves to reduce the charge separation. Although the theoretical studies seem capable of predicting the general trends in the dipole moments (except for the classical electrostatic model, which arrives at the wrong sign for the $\tilde{B}\,^2\Sigma^+$ state), none is sophisticated enough to achieve quantitative accuracy.

The $\tilde{A}$–$\tilde{X}$ and $\tilde{B}$–$\tilde{X}$ transitions of the alkaline earth monohydroxides shift progressively to the red as the group is descended. For BaOH this moves the $\tilde{A}\,^2\Pi$–$\tilde{X}\,^2\Sigma^+$ and $\tilde{B}\,^2\Sigma^+$–$\tilde{X}\,^2\Sigma^+$ systems well into the near-IR, with origins at 11 476 and 12 045 cm^{-1} for the two spin–orbit components of the $\tilde{A}$–$\tilde{X}$ system, and 13 200 cm^{-1} for the $\tilde{B}$–$\tilde{X}$ system [166–168]. Perturbations in the spectra, resulting from the close proximity of the $\tilde{A}$ and $\tilde{B}$ states, coupled with the rather inconvenient wavelengths for dye laser excitation, have limited the amount of spectroscopic work carried out on the two lowest-lying electronic transitions of BaOH.

Finally, we note that the lowest $^2\Delta$ state has been observed for two of the alkaline earth monohydroxides, CaOH and BaOH. For CaOH, excitation to this state, which lies well above the $\tilde{A}\,^2\Pi$ and $\tilde{B}\,^2\Sigma^+$ states, is vibronically induced. A high-resolution LIF study by Jarman and Bernath [169] yielded a variety of data on

the $^2\Delta$ state of CaOH, including an analysis of the Renner–Teller effect. Less detailed information is available for the lowest $^2\Delta$ state of BaOH [167]. However, it has been established that this is the lowest excited electronic state of BaOH. The marked difference between CaOH and BaOH has been attributed to dominant 5d character in the low-lying excited electronic states of BaOH. The $^2\Delta$–$^2\Pi$–$^2\Sigma^+$ trio therefore form a 'd-complex' and, since electron–electron repulsion follows the trend $d\delta < d\pi < d\sigma$, the observed state ordering is readily explained.

5.2.3. *MCp and MPy*

The binding of metal atoms to unsaturated cyclic hydrocarbons is an important phenomenon in organometallic chemistry. The alkaline earth metallocenes ($M(C_5H_5)_2$) are well-known sandwich compounds. If one of the cyclopentadienyl (Cp) ligands is stripped away, the 'half-sandwich' free radical MCp is left behind. Although much larger than the other free radicals described in the previous sections, the electronic structure in the vicinity of the metal atom should be rather similar, that is ionic bonding is expected, at least for the heavier metals, with the unpaired electron localized on the metal atom. It should therefore be feasible to observe these half-sandwich species using LIF spectroscopy in wavelength regions similar to those seen for other ML radicals.

The first successful experiments were carried out by O'Brien and Bernath [170]. Using the Broida oven technique, CaCp and SrCp were prepared and detected. The LIF spectra consisted of broad bands, with full widths at half-maximum of approximately 50 cm^{-1}. Nevertheless, the resolution was sufficient

(i) to identify the first and second excited electronic states,
(ii) to determine that the first excited state was subject to spin–orbit splitting, and
(iii) to identify structure in the M—Cp stretching mode.

The observation of spin–orbit coupling in the $\tilde{\mathbf{A}}$ state is highly significant since it confirms that the metal atom must reside above the centre of the ring (C_{5v} point-group symmetry). In no other binding site would the symmetry be high enough for the unpaired electron to retain its orbital angular momentum. By analogy with the smaller ML radicals, the metal atom donates an electron to the Cp ring, specifically the π system, yielding M^+Cp^-. The lowest lying electronic states are expected to be the $\tilde{\mathbf{X}}\,^2A_1$, $\tilde{\mathbf{A}}\,^2E$ and $\tilde{\mathbf{B}}\,^2A_1$ states. Confirmation of these symmetry assignments was derived from a rotationally resolved LIF study of CaCp [171].

Substituting the pyrollyl ligand (Py), a five-membered ring with the N atom in place of one of the CH groups in Cp, Bopegedera *et al.* [172] observed LIF spectra of CaPy and SrPy similar to those of CaCp and SrCp. Ostensibly, the metal atom has the option of binding to the ring or to the N atom, in the latter case forming the equivalent of a metal monoamide. On the basis of the apparent retention of spin–orbit splitting in the first excited electronic state, the conclusion was drawn that the metal atom remains above the ring and experiences a C_{5v} pseudosymmetry.

Subsequent jet-cooled LIF experiments by Robles *et al.* [23] on both CaCp and CaPy radicals have provided far more detailed electronic spectra. Relatively large molecules such as these are examples where supersonic cooling pays particular dividends. In the case of CaCp, the simple structure seen in the very-low-resolution excitation spectrum obtained by O'Brien and Bernath was transformed into a relatively complex spectrum at the much higher resolution of the jet-cooled experi-

ment. Although the key conclusions of the earlier work were unchanged, much new information was obtained, including the assignment of Jahn–Teller active intra-ring modes.

From the laser excitation spectra of jet-cooled CaPy the assumption by Bopegedera *et al.* that the Ca atom experiences C_{5v} pseudosymmetry was shown to be incorrect. Instead, three distinct electronic systems were observed in place of the two for CaCp because of the resolution of the $\tilde{A}\,^2E$ state into $^2A'$ and $^2A''$ states under the lower symmetry (C_s) environment of CaPy. Nevertheless, the vibrational structure was shown to be consistent with a ring-bound Ca atom in both cases. Similar findings were also reported for the monomethyl-substituted derivative of CaCp, CaMeCp [23].

Jet-cooled LIF spectra of MgCp, MgPy, and MgMeCp have also been recorded by Robles *et al.* [22]. To date, this is the only experimental study of these molecules. These molecules appear to show rather different behaviour from their Ca analogues, as befitting the much less electropositive Mg atom. In all three cases the Mg atom appears to still be located above the ring. However, the spectrum of the lowest energy electronic transition has been interpreted in terms of a metal ligand charge transfer. The approximate MO diagram of MgCp in figure 9 shows the basic idea. Because of the much larger ionization energy of Mg (7.644 eV) compared with the heavier alkaline earth metals, the 3s and 3p orbitals are closer in energy to the π orbitals of Cp. As a result, a much stronger covalent contribution to the bonding occurs, so much so that it is probably inaccurate to describe the unpaired electron as being in a metal-localized orbital in the ground electronic state. The charge-transfer transition involves excitation of an electron from the $1e_1$ orbital, nominally part of the Cp π system, to the $2a_1$ highest occupied molecular orbital (HOMO). Excitation

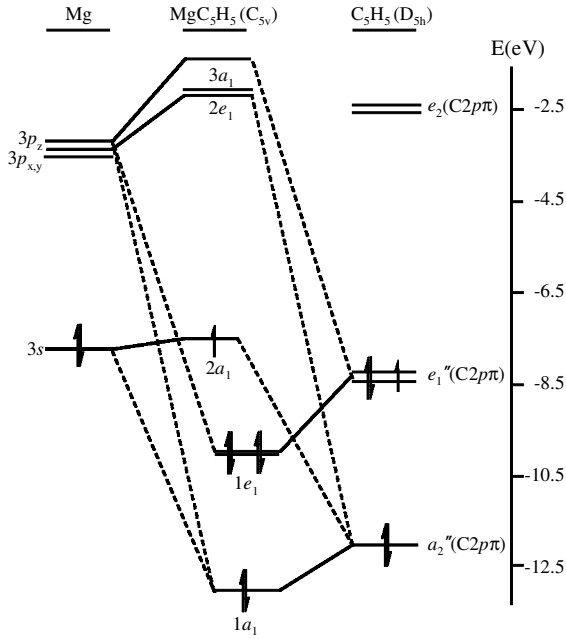

Figure 9. Approximate molecular orbital diagram for MgCp. The energy scale on the right-hand side is derived from the ionization energies of Mg and the C_5H_5 radical.

to the more strongly metal-localized $2e_1$ and $3a_1$ orbitals, which are approximately Mg 3p in character, would be the analogue of the transitions observed in CaCp and SrCp. However, in MgCp these transitions are expected to be shifted well into the UV and have not so far been detected.

6. Experimental studies of higher electronic states of alkaline-earth-containing radicals: the ligand begins to play a role

6.1. *Background*

Relatively little is known about the excited electronic states of polyatomic ML radicals outside the lowest $^2\Pi$-$^2\Sigma^+$-$^2\Delta$ manifold. Fortunately, many additional states have been observed for the alkaline earth monohalides, and these can provide useful insight into the behaviour of polyatomic species. The most extensive work has been carried out by Field *et al.* [173–180], who have investigated both valence and Rydberg states in a range of alkaline earth monohalides. In a sense, all the known states, even the ground electronic state, can be treated as members of Rydberg series since the unpaired electron is, at most, only marginally involved in the bonding process. Justification for this view is that all the observed Rydberg series for the alkaline earth monohalides extrapolate smoothly back to the well-known lower electronic states, including the ground electronic state [173]. In this discussion we focus on states lying nominally within the valence manifold, namely those dominated by *n*s, *n*p and $(n-1)$d character. Six electronic states fall into this category: three $^2\Sigma^+$, two $^2\Pi$ and one $^2\Delta$ state. These are the states shown in figure 6. Since we have already dealt with the $X\,^2\Sigma^+$, $A\,^2\Pi$, $B\,^2\Sigma^+$ and $B'\,^2\Delta$ states, this leaves the $C\,^2\Pi$ and $D\,^2\Sigma^+$ states.

We begin with the second excited $^2\Pi$ state: the $C\,^2\Pi$ state. Significant differences between this and the $A\,^2\Pi$ state in alkaline earth monohalides are apparent from a comparison of their spectroscopic constants [181]. For example, the harmonic vibrational frequency is substantially lower than in the ground electronic state, in contrast with the $A\,^2\Pi$ and $B\,^2\Sigma^+$ states for which small changes are seen. Even more striking is the variation in spin–orbit splitting. For the $A\,^2\Pi$ state this splitting is approximately invariant to the identity of the halide. In contrast the spin–orbit splitting in the $C\,^2\Pi$ state depends strongly on the halogen, increasing markedly as the group is descended. For example, in SrF the spin–orbit splitting is $64\,cm^{-1}$, whereas for SrBr this rises to $322\,cm^{-1}$ [181]. This clearly demonstrates that the unpaired electron is affected by the identity of the ligand, that is it is no longer valid to assume that the unpaired electron is in a non-bonding orbital remote from the ligand.

Information on the distribution of the spin density in the $C\,^2\Pi$ state has been extracted from experimental measurements. Ernst *et al.* [182] employed optical–microwave double resonance to determine hyperfine structure in the $C\,^2\Pi$ state of BaI. From a measurement of the Fermi contact interaction it was deduced that the unpaired electron resides in a p–d hybrid π orbital on Ba^+ with lobes distorted *towards* the I^-. Further support for this view of the $C\,^2\Pi$ state emerged from a measurement of the dipole moment of CaF by Ernst and Kändler [183] using optical Stark spectroscopy. A dipole moment of $2.45 \pm 0.06\,D$ was obtained for the $A\,^2\Pi$ state, whereas $9.24 \pm 0.17\,D$ was found for the $C\,^2\Pi$ state. This demonstrates categorically that the unpaired electron is polarized towards the ligand in the $C\,^2\Pi$ state. In this orientation there is no concentration of negative charge on the far side

of the metal to counterbalance that of the ligand, and therefore the dipole moment rises dramatically. Note that, although the π orbital is oriented towards the ligand and is therefore well placed for overlap with ligand orbitals, it appears that the metal–ligand bonding is still predominantly ionic. *Ab initio* calculations [91], as well the classical electrostatic and ligand field models [91–93, 101], are in broad agreement on this point.

The reverse polarization in the $C\,^2\Pi$ state has been attributed to an orthogonality requirement for the π orbitals in the $C\,^2\Pi$ and $A\,^2\Pi$ states. If these orbitals possess similar atomic orbital compositions, then to be orthogonal they must have opposite orientations. This is illustrated pictorially in figure 5. The weakening of the M—L bond in the $C^2\,\Pi$ state can then be explained in terms of the shielding of the M^{2+} ion from L^- by the increased electron density between these ions.

The unpaired electron density in the $D\,^2\Sigma^+$ state of alkaline earth monohalides appears to be far more diffuse than in the lower electronic states. MRDCI calculations on CaF show the spin density extending out to more than twice the distance seen in the two lower $^2\Sigma^+$ states [91]. Although nominally a valence state, Gittins *et al.* [184] have concluded that it possesses substantial Rydberg character and can therefore be regarded as a mixed valence–Rydberg state.

Armed with this information on the alkaline earth monohalides, we now move on to consider recent work on new excited electronic states of several polyatomic ML radicals.

6.2. *CaOH*

Pereira and Levy [185] presented an important new study of CaOH in 1996. Their work was the first to report electronic states above the already well-known $\tilde{\mathbf{X}}\,^2\Sigma^+$, $\tilde{\mathbf{A}}\,^2\Pi$, $\tilde{\mathbf{B}}\,^2\Sigma^+$ and $\tilde{\mathbf{C}}\,^2\Delta$ states. Both LIF and REMPI spectra revealed three new electronic states in the 28 000–31 000 cm^{-1} region. Clearly resolved rotational structure was only observed for the lowest system and showed definitively that the $\tilde{\mathbf{D}}$ state has $^2\Sigma^+$ symmetry. The assignments were less certain for the other two states, but rotational contours indicated that the $\tilde{\mathbf{E}}$ state is also a $^2\Sigma^+$ state. Most interesting was the $\tilde{\mathbf{F}}$ state, in which CaOH appears to adopt a nonlinear equilibrium geometry. The principal evidence for this was the observation of quite extensive bending mode structure in the $\tilde{\mathbf{F}}$-$\tilde{\mathbf{X}}$ emission spectrum. It therefore appears that there is a substantial degree of covalent character in the Ca—OH bonding in the $\tilde{\mathbf{F}}$ state, since a linear structure would be expected in the highly ionic limit.

The correlation between these new states of CaOH and those of the calcium monohalides is not immediately apparent. It is interesting that Pereira and Levy found no evidence in their CaOH spectra for the analogue of the $C\,^2\Pi$ state of the calcium monohalides. As will be described in the next section, the equivalent states in SrOH and BaOH have been detected. A possible explanation is that reverse polarization favours a bent geometry in CaOH, and therefore the $\tilde{\mathbf{F}}$ state is one of the two distinct electronic states that would result from the loss of orbital degeneracy. Ortiz [130] has carried out electron propagator calculations on CaOH assuming a linear geometry and predicted an energy for the reverse-polarized $^2\Pi$ state which is close to that observed for the $\tilde{\mathbf{F}}$ state. Given the comments made earlier concerning the alkaline earth monohalides it is a little surprising that sufficient covalent character could emerge from the reverse polarization of the π-like metal orbitals to cause the molecule to become bent. However, in the absence of further data this would seem to be the most likely explanation.

6.3. *SrOH and BaOH*

Although the $\tilde{A}\,^2\Pi$-$\tilde{X}\,^2\Sigma^+$ and $\tilde{B}\,^2\Sigma^+$-$\tilde{X}\,^2\Sigma^+$ systems of SrOH have been studied rather extensively (see section 5.2.2), until recently there were no reports of higher electronic transitions of this molecule. The situation has now been transformed with the identification of four new electronic systems, the $\tilde{C}\,^2\Pi$-$\tilde{X}\,^2\Sigma^+$, $\tilde{D}\,^2\Sigma^+$-$\tilde{X}\,^2\Sigma^+$, $\tilde{E}\,^2\Sigma^+$-$\tilde{X}\,^2\Sigma^+$ and $\tilde{F}\,^2\Pi$-$\tilde{X}\,^2\Sigma^+$ transitions, from work carried out in our laboratory [86]. All four systems yield strong LIF spectra in the near-UV. At the vibrationally resolved level the $\tilde{D}$-$\tilde{X}$, $\tilde{E}$-$\tilde{X}$ and $\tilde{F}$-$\tilde{X}$ systems are relatively simple to interpret. All three show structure in the Sr—O stretch only. For the $\tilde{D}$-$\tilde{X}$ and $\tilde{E}$-$\tilde{X}$ systems the Sr—O stretching progressions are much longer than is typical for the lower-lying transitions in alkaline-earth-containing free radicals. Consistent with this are substantially higher Sr—O stretching frequencies for these excited states compared with the ground electronic state, as can be seen in table 2. This can be attributed to a reduction in shielding by the electron density in the interbond region brought about by an increase in Rydberg character in these excited electronic states.

The $\tilde{C}\,^2\Pi$-$\tilde{X}\,^2\Sigma^+$ system is very different from the other three new systems, showing far more complex vibrational structure. In fact it has proved impossible, so far, to assign all the vibrational structure. However, a preliminary interpretation has emerged from a combination of rotational structure analysis and dispersed fluorescence measurements and will be outlined here.

Figure 10 shows a low-resolution survey scan of the $\tilde{C}$-$\tilde{X}$ region. The two 0_0^0 bands, separated by a $24\,cm^{-1}$ spin–orbit splitting in the $\tilde{C}\,^2\Pi$ state, are easily identified in the spectrum. We have invoked a combination of Renner–Teller coupling and Fermi resonance to explain the complex structure seen at higher energies. Central to this explanation is the apparent activity of the bending mode in the spectrum. It may at first seem surprising to invoke the bending mode when SrOH is known to be linear at equilibrium in its ground electronic state and must also be linear in the $\tilde{C}\,^2\Pi$ state given the clear observation of spin–orbit splitting (which would be quenched if the SrOH were nonlinear). According to the Franck–Condon principle, little activity in the bending mode would be expected if the molecule remains linear in both upper and lower electronic states. However, there is no doubt that the bending mode is highly active in the $\tilde{C}$-$\tilde{X}$ spectrum, as can easily be seen by inspection of dispersed fluorescence spectra such as those shown in figure 11.

Table 2. Sr—O stretching frequencies in various electronic states of SrOH[a].

Electronic state	Stretching frequency (cm^{-1})
$\tilde{X}\,^2\Sigma^+$	528[a]
$\tilde{A}\,^2\Pi$	544[a]
$\tilde{B}\,^2\Sigma^+$	522[b]
$\tilde{C}\,^2\Pi$	(535)[c]
$\tilde{D}\,^2\Sigma^+$	630[d]
$\tilde{E}\,^2\Sigma^+$	612[d]
$\tilde{F}\,^2\Pi$	(592)[e]

[a]From [162].
[b]From [164].
[c]Tentative value from [88].
[d]From [86].
[e]Tentative value from [86].

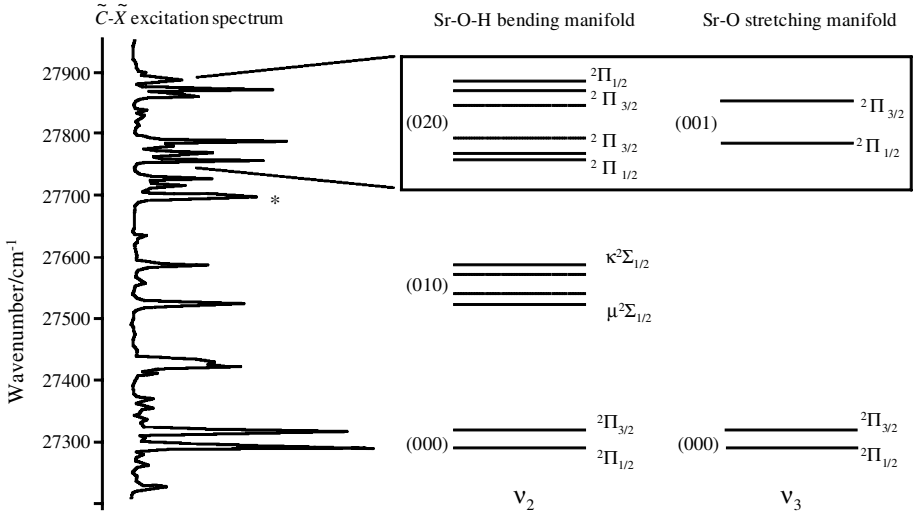

Figure 10. $\tilde{C}\,^2\Pi$-$\tilde{X}\,^2\Sigma^+$ laser excitation spectrum of SrOH. All transitions are assumed to originate from the zero point level of the $\tilde{X}\,^2\Sigma^+$ state, and the upper state symmetries shown in the figure are *vibronic* symmetries. The band indicated by an asterisk is part of the $\tilde{D}\,^2\Sigma^+$-$\tilde{X}\,^2\Sigma^+$ system. For further details see [86].

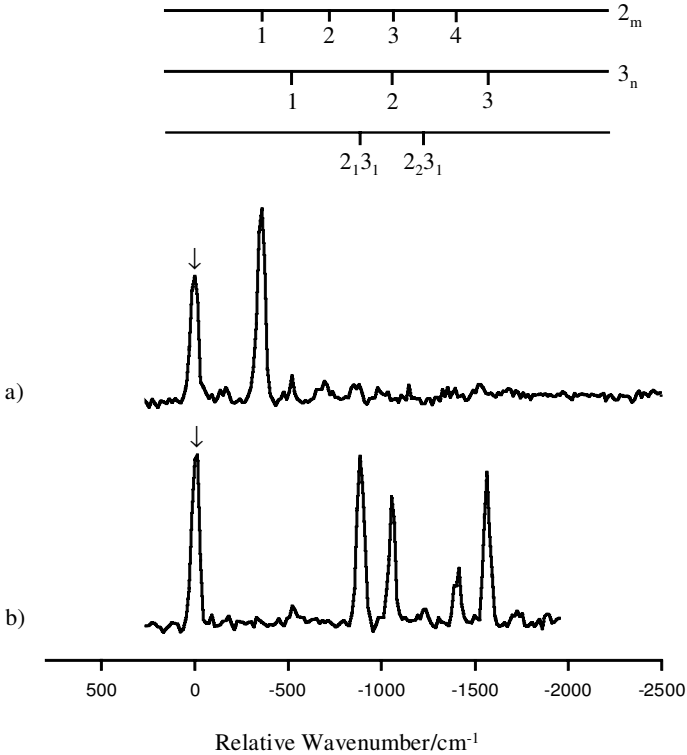

Figure 11. Dispersed fluorescence spectra of SrOH. Modes ν_2 and ν_3 refer to the SrOH bend and Sr—O stretch respectively. These spectra were obtained by excitation of the two Renner–Teller components of $\nu_2 = 1$ in the $\tilde{C}\,^2\Pi$ state, from the $\mu\,^2\Sigma^{(-)}$ (010) level (a) and from the $\kappa\,^2\Sigma^{(+)}$ (010) level (b).

The explanation is that the Franck–Condon principle breaks down owing to the Renner–Teller effect. The $\tilde{C}\,^2\Pi$ state of SrOH has a reverse-polarized unpaired electron distribution, in which the π orbital is polarized towards the O atom. The bending vibration is dominated by motion of the H atom, and therefore, the closer the unpaired electron is to the OH group, the greater is the likelihood of coupling between the orbital and vibrational angular momenta. In the $\tilde{A}\,^2\Pi$ state this is known to be small, but in the $\tilde{C}\,^2\Pi$ state it is expected to be substantially larger. In addition, a much larger dipole moment is expected for the $\tilde{C}\,^2\Pi$ state compared with the lower energy electronic states. Bolman and Brown [186] have shown that the intensity of Renner–Teller active vibrational fundamental bands in electronic spectra is proportional to the square of the difference in the dipole moments between the upper and lower electronic states. We have invoked this mechanism to account for the pronounced activity observed in the bending mode in the $\tilde{C}\,^2\Pi$–$\tilde{X}\,^2\Sigma^+$ spectrum of SrOH. The vibronic assignment is summarized in figure 10.

Transitions to the reverse-polarized $\tilde{C}\,^2\Pi$ state of BaOH have also been observed [187]. As for SrOH, the $\tilde{C}$–$\tilde{X}$ LIF spectrum was very different from other known electronic spectra of BaOH. To explain some of the features a substantial Renner–Teller effect was invoked, but the current assignment of the spectrum is tentative and further work is needed before any firm conclusions can be reached about the properties of the $\tilde{C}\,^2\Pi$ state of this molecule.

6.4. *CaNC and SrNC*

The change from relatively simple behaviour in low-lying electronic states, to rather complicated behaviour in higher states, is best illustrated by the CaNC and SrNC free radicals. Here the complications arise not only from the polarization of metal-localized orbitals but also from the orientation of the ligand. For OH it is obvious that an alkaline earth atom will bind to the O atom rather than to the H atom, since the O atom contains virtually all the excess negative charge. Based on the relative electronegativities of N and C, the metal atom is more likely to bind to the N atom when the cyanide ligand is attached, thus yielding the metal isocyanide. However, the difference in the electronegativities is not large and it is conceivable that the preferred binding site could change on electronic excitation.

This does not occur for the two lowest energy electronic transitions of CaNC and SrNC. The $\tilde{A}\,^2\Pi$–$\tilde{X}\,^2\Sigma^+$ systems for both molecules have been well characterized via LIF spectroscopy. It has been firmly established that these spectra arise from transitions in the metal isocyanide, the molecule remaining linear in both electronic states [3, 39, 45, 188]. The $\tilde{B}$–$\tilde{X}$ systems of CaNC and SrNC have also been reported and, although they have not been studied at the level of detail applied to the $\tilde{A}$–$\tilde{X}$ systems, the evidence points towards a linear–linear transition [188].

We have recently discovered several new electronic transitions of CaNC and SrNC, and these spectra are remarkably different from the lower-lying transitions [89, 189]. An example is the $\tilde{D}$–$\tilde{X}$ spectrum of SrNC shown in figure 12. This excitation spectrum shows extensive vibrational structure, with an obvious low-frequency progression. This progression is due to excitation of the bending vibration. We therefore conclude that the structure of SrNC must change on electronic excitation, since such an extensive progression in the bending mode could not occur for a linear–linear transition. In fact the spectrum has been assigned to the $\tilde{D}\,^2A'$–$\tilde{X}\,^2\Sigma^+$ system, the molecule adopting a nonlinear equilibrium structure in the excited electronic state [89]. What is particularly interesting about this spectrum

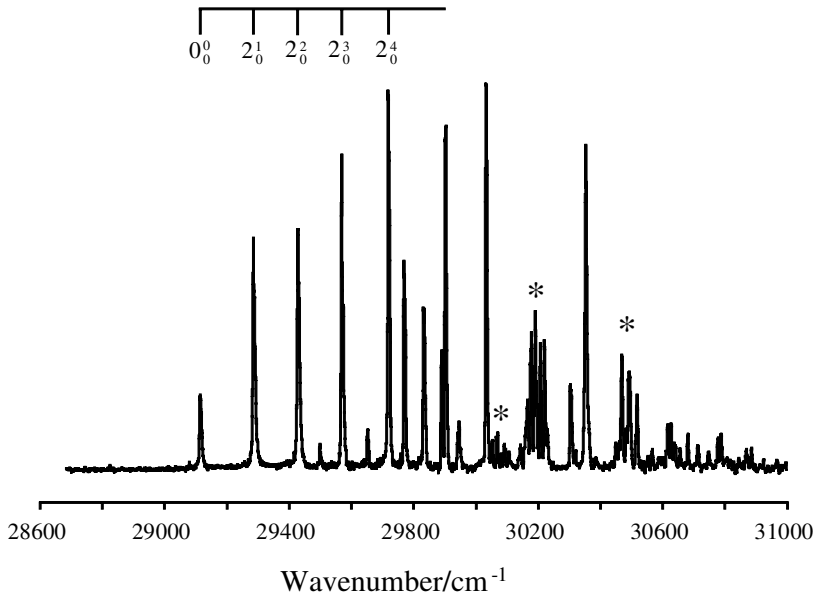

Figure 12. Laser excitation scan of the $\tilde{D}$-$\tilde{X}$ region of SrNC. Mode ν_2 is the bending vibration. The features indicated by asterisks, which are clusters of closely spaced peaks, are attributed to transitions to bending levels close to the barrier for photoisomerization. (Reproduced from [89] with the permission of the American Institute of Physics.)

is the appearance of additional bands at higher wavenumbers. Some of these occur in clusters of closely spaced peaks and have been tentatively attributed to closely spaced bending vibrational levels near to the isomerization barrier. Although the relative band intensities are different, a similar vibrational structure is observed for the $\tilde{D}$-$\tilde{X}$ system of CaNC.

Why should the structure change on excitation to the $\tilde{D}$ state? Clues come from a comparison with the alkali monoisocyanides. Analysis of pure rotational spectra of these molecules reveals that LiNC is linear whereas for Na and K a T-shaped equilibrium structure is found [190–192]. The explanation for this structural change is the increasing ionic character in the metal-ligand bond as group 1 is descended [193]. The negative charge on CN resides in a σ orbital, and therefore the Coulombic attraction between M^+ and CN^- is a maximum when the molecule is linear. In contrast, exchange repulsion is a minimum for a T-shaped structure. In LiNC, the small size of the cation allows the CN^- to approach rather closely without generating excessive exchange repulsion. As a result a linear structure is adopted, although the molecule is highly floppy in the bending coordinate. For the larger alkali atoms, exchange repulsion means that the CN^- is not able to approach the alkali cation as closely as for Li^+ in a linear configuration. The balance of forces now favours a T-shaped structure, although once again these molecules are very floppy with respect to the bending coordinate.

We can extend these arguments to the alkaline earth monoisocyanides. In doing so, it is interesting to note that *ab initio* calculations predict a T-shaped equilibrium structure for $CaNC^+$ [194]. This can be rationalized using comparable arguments with those made above for the alkali cyanides. On the other hand, neutral CaNC is

Table 3. Comparison of barriers to linearity for the alkali and alkaline earth isocyanides[a].

Isocyanide	Barrier height (cm^{-1})
CaNC	700
$CaNC^+$	800
KNC	500
SrNC	1050
RbNC	440

[a] The barrier heights for CaNC and SrNC are for the $\tilde{D}\,^2A'$ states and were deduced from the $\tilde{D}$–$\tilde{X}$ electronic spectra (see text for further details) [89]. The values for $CaNC^+$ [194], KNC [193] and RbNC [212] are estimates from *ab initio* calculations.

known to be linear in its ground state and first two excited electronic states. However, as the unpaired electron in CaNC is excited to progressively higher orbitals, at some point a switch to a T-shaped structure is expected, given the preference for a T shape in $CaNC^+$. In other words, the excitation of the electron to a sufficiently diffuse orbital will increase the Coulombic attraction between the cationic core and the CN^-, a T-shaped structure eventually being favoured in order to achieve the closest approach of the metal cation to CN^-. This mechanism appears to operate for the $\tilde{D}\,^2A'$ electronic states of both CaNC and SrNC. In fact, similar behaviour has also been found for the $\tilde{E}\,^2A'$ state of SrNC [89].

The barrier to linearity in the $\tilde{D}\,^2A'$ state can be estimated from the separation between the clusters of bands at high wavenumber and the electronic origin of the $\tilde{D}$–$\tilde{X}$ systems. If the model presented above is reasonable, then barrier heights of similar magnitude to, but generally larger than, those of the corresponding alkali isocyanide would be expected. Experimental values for the barrier heights in the alkali isocyanides are not available, but *ab initio* estimates have been obtained. Table 3 shows these data and a comparison with the barrier heights that we estimate for the $\tilde{D}\,^2A'$ states of CaNC and SrNC fits well with the preceding arguments.

To close this section, we turn to the $\tilde{C}$–$\tilde{X}$ systems of these molecules. We saw in the previous section that the $\tilde{C}$ states of SrOH and BaOH correspond to reverse-polarized $^2\Pi$ states. The electronic spectra involving these states were rather unusual and so a comparison with the $\tilde{C}$–$\tilde{X}$ spectra of the alkaline earth monoisocyanides would be interesting. The $\tilde{C}$–$\tilde{X}$ spectra of CaNC, SrNC and BaNC were first observed in 1976 in an LIF study by Pasternack and Dagdigian [196]. These spectra were largely broad and unrevealing, although there was some indication of structure for SrNC. No other work on these band systems was attempted until a recent study originating from our laboratory. Using a supersonic jet in place of the high-temperature source employed by Pasternack and Dagdigian, we were able to resolve extensive vibrational structure for one of the alkaline earth isocyanides, SrNC (see figure 13) [189].

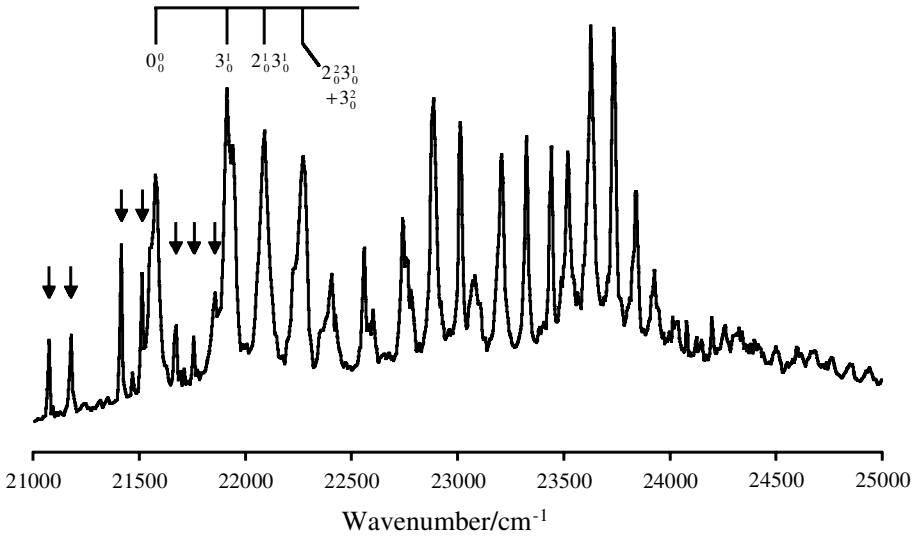

Figure 13. Jet-cooled LIF excitation spectrum of SrNC in the $\tilde{C}$-$\tilde{X}$ region. The narrow bands indicated by arrows are due to SrCCH. All other bands are due to SrNC. Modes ν_2 and ν_3 are the Sr—NC bending and stretching modes respectively. (Reproduced from [189] with permission from Elsevier Science.)

A full assignment of the structure in figure 13 is not yet available. The bands do not fit neatly into regular progressions, and there is evidence of unresolved overlapping transitions, particularly at the low-wavenumber end of the spectrum. However, it is clear that the Sr—NC stretch and the SrNC bending vibrations must both be highly active to account for the abundance and density of the observed bands. It can be concluded that, as for the $\tilde{D}$ and $\tilde{E}$ states, a bent excited-state equilibrium structure is responsible. In the linear molecule limit the $\tilde{C}$ state will be a $^2\Pi$ state. However, as the molecule is bent, this will resolve into two distinct states having $^2A'$ and $^2A''$ symmetries. It is possible that transitions to both of these states contribute to the spectrum in figure 13, but confirmation (or otherwise) requires higher-resolution spectra.

In contrast with the $\tilde{D}$-$\tilde{X}$ spectrum, there is no evidence from figure 13 that levels near to the barrier to linearity are being populated. This suggests a much larger barrier than in the $\tilde{D}\,^2A'$ state. This is perhaps unsurprising given that the excited state(s) lies (lie) roughly midway between the more rigid linear low-lying electronic states ($\tilde{X}\,^2\Sigma^+$, $\tilde{A}\,^2\Pi$ and $\tilde{B}\,^2\Sigma^+$) and the floppy nonlinear $\tilde{D}\,^2A'$ and $\tilde{E}\,^2A'$ states. *Ab initio* calculations on the excited states would be extremely helpful in understanding the reasons for this trend. However, in the absence of such calculations we speculate that the unpaired electron occupies an orbital in the $\tilde{C}$ state that possesses little Rydberg character. Indeed it looks as if the reverse-polarized orbital may be involved in significant covalent bonding to the CN group via one of the lone pairs on the N atom, thus favouring a bent and relatively rigid structure.

7. Group 12 species: a comparison with group 2

Although nominally the final group of the transition metals, group 12 elements (Zn, Cd and Hg) are best regarded as main group metals. Whereas true transition

metals may fairly readily lose one or more d electrons in forming compounds, the d shell remains completely full in almost all known compounds involving the group 12 elements. In this regard the group 12 metals are similar to the alkaline earths in that their valence configuration is ns^2, and this similarity is reflected in the old notation for the former group, group IIB. However, this similarity between the two groups holds only to a certain extent. A notable difference is the ionization energy, which tends to be much larger for the group 12 elements. As a result, covalent contributions to the bonding in group 12 compounds should be far more prevalent than for the alkaline earths.

Given the similarities and differences between the group 2 and group 12 metals, a comparison of their monoligated radical complexes would be interesting. Spectroscopic studies on polyatomic group-12-metal-containin g free radicals in the gas phase are far fewer than for group 2 species. Indeed, no such species have so far been observed for Hg. However, the news is better for Zn and Cd, with work on their monoalkyls and monocyclopentadienyls (and derivatives) having been reported. These are reviewed below.

7.1. *Zinc and cadmium monoalkyls*

7.1.1. *$ZnCH_3$ and $CdCH_3$*

The first study of the monoalkyls of Zn and Cd dates back to 1973. Using flash photolysis of the metal dimethyls, which are volatile, commercially available compounds, Young *et al.* [197] observed transient absorption spectra which were attributed to $ZnCH_3$ and $CdCH_3$. Two band systems were observed for each molecule: one in the blue region and one deep into the near-UV. The first was attributed to the $\tilde{A}\,^2E\text{-}\tilde{X}\,^2A_1$ electronic transition, and the second to the $\tilde{B}\,^2E\text{-}\tilde{X}\,^2A_1$ system. Implicit in these labels is that the MCH_3 molecules adopt a C_{3v} point-group symmetry at equilibrium, which seems reasonable but was not proven in the study by Young *et al.* Vibrational structure was resolved but subsequent work has shown that not only was some of this structure incorrectly assigned, but also the higher-energy transition is not a $^2E\text{-}^2A_1$ transition.

Considerable time elapsed before the next spectroscopic study. In 1986, Yu *et al.* [198] detected emission from the $\tilde{A}$ states of $ZnCH_3$ and $CdCH_3$ following 193 nm photolysis of $Zn(CH_3)_2$ and $Cd(CH_3)_2$. This important piece of work paved the way for LIF studies of $ZnCH_3$ and $CdCH_3$, and the first such study on $ZnCH_3$ was reported not long after by Jackson [199]. An important finding from Jackson's [199–201] investigations was that $ZnCH_3$ is formed with a large excess of internal energy following 248 nm photolysis of $Zn(CH_3)_2$ and, unless collisionally stabilized, will quickly decompose to form Zn and CH_3.

The first study of $ZnCH_3$ and $CdCH_3$ in a supersonic jet was made by Robles *et al.* [21]. In fact, this work also reported the first laser excitation spectra of these molecules, since the slightly earlier work by Jackson was restricted to dispersed fluorescence spectra. As will be detailed below, studies of these species in supersonic jets has dramatically enhanced our understanding of these molecules, yielding well-resolved vibrational structure and making it possible to record rotationally resolved spectra. In the early supersonic jet LIF work the emphasis was on assigning spin–orbit and vibrational structure. For the most part the vibrational structure is simple, with Franck–Condon activity being restricted to the M—C stretch (ν_3) and the methyl umbrella (ν_2) vibrations. The lack of extensive progressions in either mode shows that the bonding is not altered to any great degree by the electronic transition,

and this suggests promotion of a non-bonding electron. Further confirmation was provided by rotationally resolved spectra recorded by Cerny *et al.* [16], analysis of which revealed a modest change in the equilibrium bond lengths of both $ZnCH_3$ and $CdCH_3$ on excitation to the $\tilde{A}\,^2E$ state.

The similarity with the alkaline earth containing free radicals, even down to identical symmetries for the ground state and first excited electronic states, could be taken to indicate that the valence electronic structures are very similar in the two cases. However, this does not stand up to scrutiny. Crucially, as mentioned earlier, the ionization energies of group 2 and group 12 elements differ fairly dramatically. Thus for Ca we have 6.11 eV whereas Zn has a first ionization energy of 9.39 eV. Indeed the latter is only marginally below that of methyl (9.84 eV [202]). In contrast with the analogous alkaline-earth-containing species, the bonding cannot be highly ionic in the ground electronic states of the group 12 monoalkyls.

A combination of spectroscopic data and *ab initio* calculations [203–205] point to an electronic structure represented by the molecular orbital diagram in figure 14. In this figure, it is assumed that the closed d shell makes no significant contribution to the bonding. The bonding in the ground electronic state is then dominated by the overlap of the *n*s valence orbital on the metal and the $2p_z$ orbital on the CH_3, the latter containing a single electron in the ground electronic state ($^2A_2''$) of free CH_3. The overlap of these orbitals leads to two σ-like orbitals: one bonding and the other antibonding. According to this model the unpaired electron resides in the antibonding molecular orbital. There is some debate about the character of the latter orbital. In particular, ESR spectra of $ZnCH_3$ and $CdCH_3$ in rare-gas matrices, supported by *ab initio* calculations, suggest that the dominant metal contribution is *n*p rather than *n*s [206, 207]. Whether this proportion is correct or not, it does seem likely that substantial *n*p character is present, since this will allow the orbital to polarize away from the ligand. In this scheme the HOMO is antibonding but only mildly so, since the polarization away from the ligand confers significant non-bonding character.

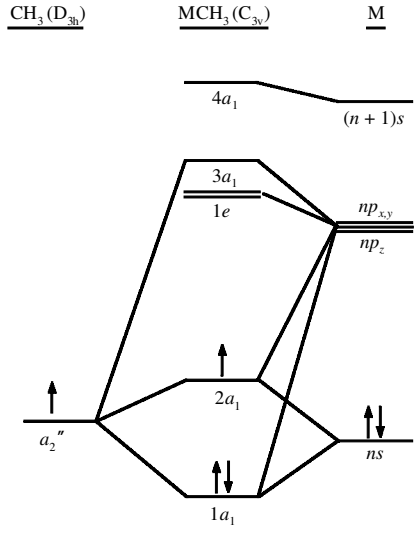

Figure 14. Qualitative molecular orbital diagram for MCH_3 (M = Zn or Cd). The single orbital contributed by CH_3 is the C 2pπ orbital oriented perpendicular to the plane containing the H atoms.

The first excited electronic state, the $\tilde{A}\,^2E$ state, is dominated by the Zn 4p orbitals. Here the unpaired electron resides in an almost completely non-bonding orbital on account of the large energy separation between the Zn 4p and C 2p orbitals. Thus the $\tilde{A}$-$\tilde{X}$ transition involves the unpaired electron moving from a mainly Zn-localized, mildly antibonding molecular orbital ($2a_1$) to an almost completely non-bonding Zn-localized (4p) orbital (1e). Support for this model is legion. For example, the M—C stretching vibrational frequencies increase, and the M—C equilibrium bond lengths decrease, on electronic excitation. However, these changes are fairly modest, supporting the suggestion that the transition involves a mild change in bonding character. Furthermore, spin–orbit splitting in the $\tilde{A}\,^2E$ state of $ZnCH_3$ is observed with a magnitude compatible with strong 4p character for the unpaired electron [21].

Very recently, Miller's research group have reported fascinating new studies on $ZnCH_3$ and $CdCH_3$ that have further deepened our understanding of these molecules. Two new techniques have been brought to bear: zero-electron-kinetic-energy (ZEKE) spectroscopy and fluorescence depletion (FD) spectroscopy. The ZEKE work provided the first experimental information on the cations [17, 18]. It also provided data on the vibrations active in the neutral molecule LIF spectra. The previous assignments of vibrational structure in the two totally symmetric modes ν_2 and ν_3 were found to be correct. However, additional bands in both $ZnCH_3$ and $CdCH_3$ spectra were reassigned to the doubly degenerate methyl rocking mode ν_6 which gains its activity through a modest Jahn–Teller effect.

In a beautiful piece of work, Pushkarsky *et al.* [19] used FD spectroscopy to access 'dark' levels of $CdCH_3$, that is excited-state levels that do not fluoresce. Previous work had shown that no rovibrational levels in the $\tilde{A}\,^2E_{3/2}$ manifold fluoresce [18], and in addition the fluorescence quantum yield in the $\tilde{A}\,^2E_{1/2}$ manifold falls off rapidly as the vibrational energy is increased [208]. FD spectroscopy is a two-laser technique in which the population of dark levels, achieved by laser 1, is monitored by detecting fluorescence from bright states populated by laser 2. Resonant excitation of dark levels is observed as dips in the fluorescence intensity. An array of new levels in both the $\tilde{A}\,^2E_{1/2}$ and $\tilde{A}\,^2E_{3/2}$ manifolds were found by Pushkarsky *et al.* using this approach. Most of these were accounted for in terms of three modes: the Cd—C stretch, the methyl umbrella and the Jahn–Teller-induced methyl rocking mode. The prominence of ν_6, the methyl rocking mode, in the FD spectrum has been tentatively assigned to insertion of Cd into one of the C—H bonds as ν_6 is excited, thus efficiently quenching the fluorescence.

7.1.2. *ZnC_2H_5 and CdC_2H_5*

Given the successful spectroscopic detection of $ZnCH_3$ and $CdCH_3$, it seems reasonable to search for spectra of the heavier zinc and cadmium monoalkyls. The latter will present new challenges, not least because their lower symmetries will remove the electronic and vibrational degeneracies observed for $ZnCH_3$ and $CdCH_3$. The first attempt to record such spectra was reported in 1992 by Jackson [200]. Using a similar approach to his earlier LIF work on $ZnCH_3$, Jackson sought LIF spectra of zinc monoethyl and zinc monoisopropyl by photolysing the corresponding zinc dialkyls at 248 nm in the presence of an inert buffer gas. No spectra were observed. This was attributed to the higher density of states in these molecules compared with $ZnCH_3$ and $CdCH_3$, leading to rapid non-radiative relaxation in the excited electronic state.

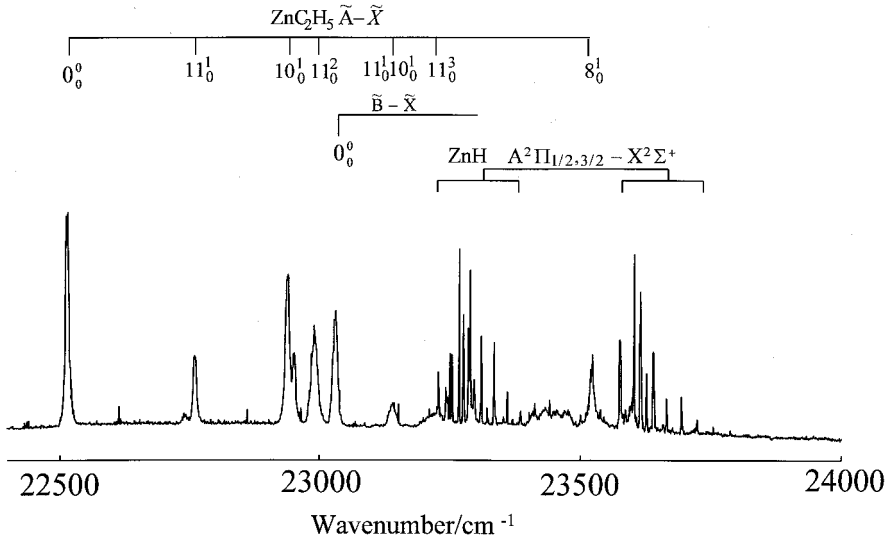

Figure 15. Laser excitation spectrum of ZnC_2H_5. (Reproduced from [209] with permission from Academic Press).

Two years later we showed that this conclusion is erroneous, at least in the case of ZnC_2H_5. Not only does this molecule fluoresce, but also it does so with a very high fluorescence quantum yield [76]. Our initial work involved a pulsed electrical discharge method to produce the ZnC_2H_5 radical from the $Zn(C_2H_5)_2$, but subsequent work showed that 193 or 248 nm photolysis is also effective. The vibrationally resolved laser excitation spectrum of ZnC_2H_5 is shown in figure 15. Most of the spectral assignments were made on the basis of dispersed fluorescence data, supplemented by *ab initio* calculations [209]. Several modes are active in the spectrum, but most of the prominent structure arises from the Zn—C stretching and Zn—C—C bending modes ν_{10} and ν_{11} respectively. These are expected to be the primary active modes if the electronic transition is largely metal localized. The Zn—C stretch has a lower frequency than in $ZnCH_3$, but the reduction is largely in line with that expected on the basis of a reduced mass effect alone. Furthermore, the $\tilde{A}$-$\tilde{X}$ 0_0^0 transition is only (red) shifted some 1600 cm^{-1} from that of $ZnCH_3$. These data taken together show that substitution of C_2H_5 for CH_3 has a significant but not major impact on the electronic structure of the lowest-lying electronic states.

Observation of LIF spectra of CdC_2H_5 is more difficult. Diethyl cadmium, unlike diethyl zinc, undergoes rapid thermal decomposition at or near room temperature and is therefore unsuitable as a photolysis or discharge precursor of CdC_2H_5. However, we succeeded in making this radical by Cd atom reactions within the dual-channel discharge nozzle described in section 2.1 [210]. The laser excitation spectrum is weak and consists of only a single band assigned to the $\tilde{A}$-$\tilde{X}$ 0_0^0 transition. Dispersed fluorescence spectra support this assignment, showing vibrational structure in three modes: the Cd—C stretch, the Cd—C—C bend and the C—C stretch. Although the low intensity of the LIF spectrum of CdC_2H_5 compared with ZnC_2H_5 may be due in part to inefficient production of the former, it also seems likely that the fluorescence quantum yield is low. LIF experiments have not been

attempted on the heavier zinc and cadmium monoalkyls but these findings for CdC_2H_5 are not encouraging, suggesting that non-radiative relaxation may become a severe obstacle for the heavier species.

Very recent work from Miller's group at Ohio State University looks likely to improve our understanding of the geometry and electronic structure of ZnC_2H_5. Rotationally resolved laser excitation spectra have been recorded, although a full analysis has proved difficult and is not yet available. When complete, this should provide a wealth of new information, including a firm assignment of excited state symmetries. ZEKE spectra have also recently been recorded for ZnC_2H_5 [20].

To close this section it is worth noting that, while electronic spectra of the monomethyls of the group 2 metals Mg, Ca and Sr have been recorded, the analogous spectra of the group 2 monoethyls have not been observed, despite attempts by our group and others to do so.

7.2. *Zinc and cadmium monocyclopentadienyls and monopyrollyls*

The only other polyatomic Zn- and Cd-containing free radicals that have been identified by electronic spectroscopy in the gas phase are ZnCp and CdCp, together with their monosubstituted derivatives ZnPy, ZnMeCp, CdPy and CdMeCp [4, 25, 26]. The first ionization energies of both Zn and Cd are larger than that of Cp (8.4 eV [211]), suggesting that covalent bonding will play a vital role in these molecules. In fact, as befitting these large metal ionization energies, the bonding and spectra have more in common with MgCp than with the highly ionic CaCp and SrCp radicals. As for MgCp, the lowest electronic transition is believed to be a metal ligand charge transfer transition. Electron propagator calculations by Zakrzewski and Ortiz [212] support this conclusion. The metal atom resides above the centre of the five-membered ring, making the lowest transition the $\tilde{A}\,^2E_1$–$\tilde{X}\,^2A_1$ transition. Despite the orbital degeneracy in the excited state, no spin–orbit coupling is resolved in the LIF spectra because the spin–orbit coupling constant is characteristic of the C $2p_\pi$ system on Cp, on which the unpaired electron resides.

Dramatic confirmation of this is provided by substitution of Py or MeCp in place of Cp. For both Zn and Cd, two closely spaced but very distinct electronic band systems appear owing to the loss of the excited electronic state degeneracy seen for ZnCp and CdCp [26]. Detailed analyses of the vibrational structure in the spectra of these molecules have been performed, showing categorically that they correspond to a ring-bound metal atom.

The difference between the electronic structures of the group 12 monoalkyls and monocyclopentadienyls is due to the presence of additional valence orbitals for the latter ligand. The situation is nicely illustrated by the molecular orbital diagram for MgCp in figure 9, which also applies qualitatively to ZnCp and CdCp. The $1e_1$ orbitals on Cp, which have no equivalent in MCH_3 or MC_2H_5, do not have the correct symmetry to interact with the *n*s orbital on the metal. However, interaction with the np_π orbitals on the metal is possible, pushing the $1e_1$ orbitals down between the $1a_1$ and $2a_1$. Concomitantly, the largely metal-localized $2e_1$ orbitals, which are analogous to the HOMO in the first excited states of MCH_3 and MC_2H_5, are pushed to much higher energies [212], well beyond the regions surveyed so far for ZnCp and CdCp (and their substituted analogues).

8. Conclusions

The application of laser techniques in the study of the structure and bonding in simple ML free radicals has been described. Considerable progress has been made for molecules composed of a single group 2 or group 12 metal atom bound to small- or medium-sized ligands such as OH, CN or NC, CCH, CH_3 and C_2H_5. Vibrationally resolved spectra have been obtained for all these molecules, in some cases for several different electronic transitions. Rotationally resolved spectra have also been obtained for some of the lighter species. These spectra, together with supporting theoretical calculations where available, have provided new information on the structure and bonding.

Future challenges in this area are many. Of particular interest would be the investigation of transition-metal-containing analogues to those molecules described in this review. Little progress has been made towards this aim to date, and there are many potential obstacles. The electronic spectra of diatomic transition metal containing molecules are notoriously complex to analyse; therefore polyatomics are likely to pose an especially difficult problem. There is also the perennial limitation associated with techniques such as LIF and REMPI, namely their requirement of an excited state that does not undergo rapid non-radiative decay, otherwise it is usually rendered undetectable by either method. Furthermore, it is exceedingly time consuming to carry out extensive survey scans for electronic spectra of new species using current tunable laser systems.

Despite these difficulties, progress is being made. We note with great interest the very recent observation of FeNC by Lie and Dagdigian [213]. Using LIF spectroscopy, and guided by work carried out previously on FeCl, vibrationally and rotationally resolved electronic spectra of FeNC were obtained. This work is the first high-resolution spectroscopic study of a triatomic iron-containing molecule, and it may ultimately lead to new studies of other transition-metal-containing molecules.

Acknowledgements

It is a pleasure to be able to acknowledge those persons with whom the author has worked on the material described in this review. They include Professor T. A. Miller and Dr E. S. J. Robles at the Ohio State University and Dr M. S. Beardah, Dr A. J. Bezant, Dr G. K. Corlett, Dr G. M. Greetham, Dr A. M. Little, Dr I. M. Povey and Dr S. J. Pooley at the University of Leicester. Financial support from various sources, especially the UK Science and Engineering Research Council, is also gratefully acknowledged.

References

[1] Jacox, M. E., 1994, *Chem. Phys.*, **189**, 149.
[2] Bernath, P. F., 1991, *Science*, **254**, 665.
[3] Whitham, C. J., Soep, B., Visticot, J. P., and Keller, A., 1990, *J. chem. Phys.*, **93**, 991.
[4] Ellis, A. M., Robles, E. S. J., and Miller, T. A., 1991, *J. chem. Phys.*, **94**, 1752.
[5] Morbi, Z., Zhao, C. F., Hepburn, J. W., and Bernath, P. F., 1998, *J. chem. Phys.*, **108**, 8891.
[6] Morbi, Z., Zhao, C. F., and Bernath, P. F., 1997, *J. chem. Phys.*, **106**, 4860.

[7] Zhao, C., Hajigeorgiou, P. G., Bernath, P. F., and Hepburn, J. W., 1996, *J. molec. Spectrosc.*, **176**, 268.
[8] Smith, T. C., Clouthier, D. J., Sha, W., and Adam, A. C., 2000, *J. chem. Phys.*, **113**, 9567.
[9] Smith, T. C., Li, H. Y., Clouthier, D. J., Kingston, C. T., and Merer, A. J., 2000, *J. chem. Phys.*, **112**, 8417.
[10] Hostutler, D. A., Smith, T. C., Li, H. Y., and Clouthier, D. J., 1999, *J. chem. Phys.*, **111**, 950.
[11] Smith, T. C., Li, H. Y., and Clouthier, D. J., 1999, *J. Am. chem. Soc.*, **121**, 6068.
[12] Adam, A. G., Athanassenas, K., Gillett, D. A., Kingston, C. T., Merer, A. J., Peers, J. R. D. , and Rixon, S. J., 1999, *J. molec. Spectrosc.*, **196**, 45.
[13] Barnes, M., Merer, A. J., and Metha, G. F., 1997, *J. molec. Spectrosc.*, **181**, 168.
[14] Barnes, M., Gillett, D. A., Merer, A. J., and Metha, G. F., 1996, *J. chem. Phys.*, **105**, 6168.
[15] Barnes, M., Hajigeorgiou, P. G., Kasrai, R., Merer, A. J., and Metha, G. F., 1995, *J. Am. chem. Soc.*, **117**, 2096.
[16] Cerny, T. M., Tan, X. Q., Williamson, J. M., Robles, E. S. J., Ellis, A. M., and Miller, T. A., 1993, *J. chem. Phys.*, **99**, 9376.
[17] Barckholtz, T. A., Powers, D. E., Miller, T. A., and Bursten, B. E., 1999, *J. Am. chem. Soc.*, **121**, 2576.
[18] Panov, S. I., Powers, D. E., and Miller, T. A., 1998, *J. chem. Phys.*, **108**, 1335.
[19] Pushkarsky, M. B., Barckholtz, T. A., and Miller, T. A., 1999, *J. chem. Phys.*, **110**, 2016.
[20] Pushkarsky, M. B., Stakhursky, V. L., and Miller, T. A., 2000, *J. phys. Chem.* A, **104**, 9184.
[21] Robles, E. S. J., Ellis, A. M., and Miller, T. A., 1991, *Chem. Phys. Lett.*, **178**, 185.
[22] Robles, E. S. J., Ellis, A. M., and Miller, T. A., 1992, *J. phys. Chem.*, **96**, 8791.
[23] Robles, E. S. J., Ellis, A. M., and Miller, T. A., 1992, *J. Am. chem. Soc.*, **114**, 7171.
[24] Robles, E. S. J., Ellis, A. M., and Miller, T. A., 1992, *J. chem. Soc., Faraday Trans.*, **88**, 1927.
[25] Robles, E. S. J., Ellis, A. M., and Miller, T. A., 1992, *J. phys. Chem.*, **96**, 3247.
[26] Robles, E. S. J., Ellis, A. M., and Miller, T. A., 1992, *J. phys. Chem.*, **96**, 3258.
[27] Jakubek, Z. J., Simard, B., Niki, H., and Balfour, W. J., 2000, *J. chem. Phys.*, **113**, 3591.
[28] Jakubek, Z. K., and Simard, B. K., 2000, *J. chem. Phys.*, **112**, 1733.
[29] Simard, B., Jakubek, Z., Niki, H., and Balfour, W. J., 1999, *J. chem. Phys.*, **111**, 1483.
[30] Loock, H. P., Berces, A., Simard, B., and Linton, C., 1997, *J. chem. Phys.*, **107**, 2720.
[31] Simard, B., Balfour, W. J., Vasseur, M., and Hackett, P. A., 1990, *J. chem. Phys.*, **93**, 4481.
[32] Steimle, T. C., 2000, *Int. Rev. phys. Chem.*, **19**, 455.
[33] Namiki, K. C., Robinson, J. S. , and Steimle, T. C., 1998, *J. chem. Phys.*, **109**, 5283.
[34] Steimle, T. C., Xin, J., Marr, A. J., and Beaton, S., 1997, *J. chem. Phys.*, **106**, 9084.
[35] Marr, A. J., Grieman, F., and Steimle, T. C., 1996, *J. chem. Phys.*, **105**, 3930.
[36] Steimle, T. C., Marr, A. J., Xin, J., Merer, A. J., Athanassenas, K., and Gillet, D., 1997, *J. chem. Phys.*, **106**, 2060.
[37] Marr, A. J., Tanimoto, M., Goodridge, D., and Steimle, T. C., 1995, *J. chem. Phys.*, **103**, 4466.
[38] Marr, A. J., Perry, J., and Steimle, T. C., 1995, *J. chem. Phys.*, **103**, 3861.
[39] Scurlock, C. T., Fletcher, D. A., and Steimle, T. C., 1994, *J. chem. Phys.*, **101**, 7255.
[40] Scurlock, C. T., Henderson, T., Bosely, S., Jung, K. Y., and Steimle, T. C., 1994, *J. chem. Phys.*, **100**, 5481.
[41] Scurlock, C. T., Steimle, T. C., Suenram, R. D., and Lovas, F. J., 1994, *J. chem. Phys.*, **100**, 3497.
[42] Steimle, T. C., Scurlock, C. J., Jung, K. Y., and Henderson, T. S., 1994, *Abstr. Pap. Am. chem. Soc.*, **207**, 194.

[43] Scurlock, C. T., Fletcher, D. A., and Steimle, T. C., 1993, *J. molec. Spectrosc.*, **159**, 350.
[44] Fletcher, D. A., Jung, K. Y., Scurlock, C. T., and Stiemle, T. C., 1993, *J. chem. Phys.*, **98**, 1837.
[45] Steimle, T. C., Fletcher, D. A., Jung, K. Y., and Scurlock, C. T., 1992, *J. chem. Phys.*, **97**, 2909.
[46] Steimle, T. C., Fletcher, D. A., Jung, K. Y., and Scurlock, C. T., 1992, *J. chem. Phys.*, **96**, 2556.
[47] Thompsen, J. M., Sheridan, P. M., and Ziurys, L. M., 2000, *Chem. Phys Lett.*, **330**, 373.
[48] Sheridan, P. M., and Ziurys, L. M., 2000, *Astrophys. J.*, **540**, L61.
[49] Brewster, M. A., and Ziurys, L. M., 2000, *J. chem Phys.*, **113**, 3141.
[50] Grotjahn, D. B., Pesch, T. C., Brewster, M. A., and Ziurys, L. M., 2000, *J. Am. chem. Soc.*, **122**, 4735.
[51] Xin, J., Brewster, M. A., and Ziurys, L. M., 2000, *Astrophys J.*, **530**, 323.
[52] Xin, J., and Ziurys, L. M., 1999, *J. chem. Phys.*, **110**, 3360.
[53] Apponi, A. J., Brewster, M. A., and Ziurys, L. M., 1998, *Chem. Phys. Lett.*, **298**, 161.
[54] Xin, J., and Ziurys, L. M., 1998, *Astrophys. J.*, **508**, L109.
[55] Grotjahn, D. B., Apponi, A. J., Brewster, M. A., Xin, J., and Ziurys, L. M., 1998, *Agnew. Chem., Int. Edn*, **37**, 2678.
[56] Allen, M. D., Pesch, T. C., Robinson, J. S., Apponi, A. J., Grotjahn, D. B., and Ziurys, L. M., 1998, *Chem. Phys. Lett.*, **293**, 397.
[57] Xin, J., and Ziurys, L. M., 1998, *Astrophys J.*, **501**, L151.
[58] Xin, J., Robinson, J. S., Apponi, A. J., and Ziurys, L. M., 1998, *J chem. Phys.*, **108**, 2703.
[59] Li, B. Z., Xin, J., and Ziurys, L. M., 1997, *Chem. Phys Lett.*, **280**, 513.
[60] Grotjahn, D. B., Pesch, T. C., Xin, J., and Ziurys, L. M., 1997, *J. Am. chem. Soc.*, **119**, 12 368.
[61] Robinson, J. S., Apponi, A. J., and Ziurys, L. M., 1997, *Chem. Phys Lett.*, **278**, 1.
[62] Li, B. Z., and Ziurys, L. M., 1997, *Astrphys. J.*, **482**, L215.
[63] Robinson, J. S., and Ziurys, L. M., 1996, *Astrophys. J.*, **472**, L131.
[64] Anderson, M. A., Robinson, J. S., and Ziurys, L. M., 1996, *Chem. Phys Lett.*, **257**, 471.
[65] Anderson, M. A., and Ziurys, L. M., 1996, *Astrophys. J.*, **460**, L77.
[66] Nuccio, B. P., Apponi, A. J., and Ziurys, L. M., 1995, *Chem. Phys. Lett.*, **247**, 283.
[67] Nuccio, B. P., Apponi, A. J., and Ziurys, L. M., 1995, *J. chem. Phys.*, **103**, 9193.
[68] Bunker, P. R., Kolbuszewski, M., Jensen, P., Brumm, M., Anderson, M. A., Barclay, W. L., Ziurys, L. M., Ni, Y., and Harris, D. O., 1995, *Chem. Phys. Lett.*, **239**, 217.
[69] Anderson, M. A., and Ziurys, L. M., 1995, *Astrophys. J.*, **444**, L57.
[70] Anderson, M. A., and Ziurys, L. M., 1994, *Chem Phys Lett.*, **231**, 164.
[71] Anderson, M. A., Steimle, T. C., and Ziurys, L. M., 1994, *Astrophys. J.*, **429**, L41.
[72] Apponi, A. J., Barclay, W. L., and Ziurys, L. M., 1993, *Astrophys. J.*, **414**, L129.
[73] Anderson, M. A., Allen, M. D., Barclay, W. L., and Ziurys, L. M., 1993, *Chem. Phys. Lett.*, **205**, 415.
[74] Anderson, M. A., Barclay, W. L., and Ziurys, L. M., 1992, *Chem. Phys. Lett.*, **196**, 166.
[75] Ziurys, L. M., Barclay, W. L., and Anderson, M. A., 1992, *Astrophys. J.*, **384**, L63.
[76] Povey, I. M., Bezant, A. J., Corlett, G. K., and Ellis, A. M., 1994, *J. phys. Chem.*, **98**, 10 427.
[77] West, J. B., Bradford, R. S., Eversole, J. D., and Jones, C. R., 1975, *Rev. scient. Instrum.*, **46**, 164.
[78] Ellingboe, L. C., Bopegedera, A., Brazier, C. R., and Bernath, P. F., 1986, *Chem. Phys Lett.*, **126**, 285.
[79] Brazier, C. R., Ellingboe, L. C., Kinseynielsen, S., and Bernath, P. F., 1986, *J. Am. chem. Soc.*, **108**, 2126.
[80] Crumley, W. H., Hayden, J. S., and Cole, J. L., 1986, *J. chem. Phys.*, **84**, 5250.

[81] Grieman, F. J., Ashworth, S. H., Brown, J. M., and Beattie, I. R., 1990, *J. chem. Phys.*, **92**, 6365.
[82] Woodward, J. R., Cobb, S. H., and Gole, J. L., 1988, *J. phys. Chem.*, **92**, 1404.
[83] Zink, L. R., Brown, J. M., Gilson, T. R., and Beattie, I. R., 1988, *Chem. Phys. Lett.*, **146**, 501.
[84] Dietz, T. G., Duncan, M. A., Powers, D. E., and Smalley, R. E., 1981, *J. chem. Phys.*, **74**, 6511.
[85] Gole, J. L., English, J. H., and Bondybey, V. E., 1982, *J. phys Chem.*, **86**, 2560.
[86] Beardah, M. S., and Ellis, A. M., 1999, *J. chem. Phys.*, **110**, 11 244.
[87] Bezant, A. J., Turner, D. D., Dormer, G., and Ellis, A. M., 1996, *J. chem. Soc., Faraday Trans.*, **92**, 3023.
[88] Beardah, M. S., PhD Thesis, University of Leicester, Leicester, 1999.
[89] Greetham, G. M., and Ellis, A. M., 2000, *J. chem. Phys.*, **113**, 8945.
[90] Knight, L. B., Easley, W. C., Weltner, W., and Wilson, M., 1971, *J. chem. Phys.*, **54**, 322.
[91] Bundgen, P., Engles, B., and Peyerhimhoff, S. D., 1991, *Chem. Phys. Lett.*, **176**, 407.
[92] Torring, T., Ernst, W. E., and Kandler, J., 1989, *J. chem. Phys.*, **90**, 4927.
[93] Rice, S. F., Martin, H., and Field, R. W., 1985, *J. chem. Phys.*, **82**, 5023.
[94] Jarman, C. N., and Bernath, P. F., 1993, *J. chem. Phys.*, **98**, 6697.
[95] Ortiz, J. V., 1990, *Chem. Phys. Lett.*, **169**, 116.
[96] Rittner, E. S., 1951, *J. chem. Phys.*, **19**, 1030.
[97] Klynning, L., and Martin, H., 1980, *Physica scripta*, **22**, 221.
[98] Klynning, L., and Martin, H., 1981, *Physica scripta*, **24**, 33.
[99] Torring, T., Ernst, W. E., and Kindt, S., 1984, *J. chem. Phys.*, **81**, 4614.
[100] Mestdagh, J. M., and Visticot, J. P., 1991, *Chem. Phys.*, **155**, 79.
[101] Allouche, A. R., and Aubert-Frecon, M., 1994, *J. molec. Spectrosc.*, **163**, 599.
[102] Langhoff, S. R., Bauschlicher, C. W., Partridge, H., and Ahlrichs, R., 1986, *J. chem. Phys.*, **84**, 5025.
[103] Langhoff, S. R., Bauschlicher, C. W., and Partridge, H., 1986, *J. chem. Phys.*, **84**, 1687.
[104] Bauschlicher, C. W., Langhoff, S. R., and Partridge, H., 1985, *Chem. Phys. Lett.*, **115**, 124.
[105] Smith, J. R., Kim, J. B., and Lineberger, W. C., 1997, *Phys. Rev.* A, **55**, 2036.
[106] Klein, R., McGinnis, R. P., and Leone, S. R., 1983, *Chem. Phys Lett.*, **100**, 475.
[107] Bauschlicher, C. W., Langhoff, S. R., and Partridge, H., 1986, *J. chem. Phys.*, **84**, 901.
[108] Jain, S. K., Rout, C., and Rastogi, R. C., 2000, *Chem. Phys. Lett.*, **331**, 547.
[109] Theodorakopoulos, G., Petsalakis, I. D., and Hamilton, I. P., 1999, *J. chem. Phys.*, **111**, 10 484.
[110] Fernandez, B., 1996, *Chem. Phys. Lett.*, **259**, 635.
[111] Palke, W. E., and Kirtman, B., 1985, *Chem. Phys. Lett.*, **117**, 424.
[112] Kong, J., and Boyd, R. J., 1995, *J. chem. Phys.*, **103**, 10 070.
[113] Kong, J., and Boyd, R. J., 1996, *J. chem. Phys.*, **104**, 4055.
[114] Tyerman, S. C., Corlett, G. K., Ellis, A. M., and Claxton, T. A., 1996, *Theochem—J. molec. Struct.*, **364**, 107.
[115] Woon, D. E., 1996, *Astrophys. J.*, **456**, 602.
[116] Chan, W. T., and Hamilton, I. P., 1998, *Chem. Phys. Lett.*, **297**, 217.
[117] Chan, W. T., and Hamilton, I. P., 2000, *Chem. Phys. Lett.*, **316**, 171.
[118] Raouafi, S., Jeung, G. H., and Jungen, C., 1999, *J. molec. Spectrosc.*, **196**, 248.
[119] Machado, F. B. C., Roberto-Neto, O., and Ornellas, F. R., 1999, *Chem. Phys. Lett.*, **305**, 156.
[120] Machado, F. B. C., Roberto-Neto, P., and Ornellas, F. R., 1998, *Chem. Phys. Lett.*, **284**, 293.
[121] Leininger, T., and Jeung, G. H., 1995, *J. chem. Phys.*, **103**, 3942.
[122] Leininger, T., and Jeung, G. H., 1994, *Phys. Rev.* A, **49**, 2415.
[123] Ornellas, F. R., Machado, F. B. C., and Robertoneto, O., 1992, *Molec. Phys.*, **77**, 1169.

[124] Honjou, N., Adams, G. F., and Yarkony, D. R., 1983, *J. chem. Phys.*, **79**, 4376.
[125] Honjou, N., Takagi, M., Makita, M., and Ohno, K., 1981, *J. phys. Soc. Japan*, **50**, 2095.
[126] Bauschlicher, C. W., Langhoff, S. R., Steimle, T. C., and Shirley, J. E., 1990, *J. chem. Phys.*, **93**, 4179.
[127] Woon, D. E., 1996, *J. chem. Phys.*, **104**, 9495.
[128] Woon, D. E., 1997, *Chem. Phys. Lett.*, **274**, 299.
[129] Nanbu, S., Minamino, S., and Aoyagi, M., 1997, *J. chem. Phys.*, **106**, 8073.
[130] Ortiz, J. V., 1990, *J. chem. Phys.*, **92**, 6728.
[131] Ortiz, J. V., 1991, *J. Am. chem. Soc.*, **113**, 1102.
[132] Ortiz, J. V., 1991, *J. Am. chem. Soc.*, **113**, 3593.
[133] Ortiz, J. V., 1992, *Int. J. quant. Chem.*, 1.
[134] Thompson, C. A., and Andrews, L., 1996, *J. Am. chem. Soc.*, **118**, 10 242.
[135] Anderson, M. A., and Ziurys, L. M., 1995, *Astropys. J.*, **439**, L25.
[136] Ziurys, L. M., Apponi, A. J., Guelin, M., and Cernicharo, J., 1995, *Astrophys. J.*, **445**, L47.
[137] Kawaguchi, K., Kagi, E., Hirano, T., Takano, S., and Saito, S., 1993, *Astrophys. J.*, **406**, L39.
[138] Corlett, G. K., Little, A. M., and Ellis, A. M., 1996, *Chem. Phys. Lett.*, **249**, 53.
[139] Corlett, G. K., Beardah, M. S., and Ellis, A. M., 1997, *J. molec. Spectrosc.*, **185**, 202.
[140] Brewster, M. A., Apponi, A. J., Xin, J., and Ziurys, L. M., 1999, *Chem. Phys. Lett.*, **310**, 411.
[141] Bopegedera, A., Brazier, C. R., and Bernath, P. F., 1987, *Chem. Phys. Lett.*, **136**, 97.
[142] Bopegedera, A., Brazier, C. R., and Bernath, P. F., 1988, *J. molec. Spectrosc.*, **129**, 268.
[143] Li, M. G., and Coxon, J. A., 1996, *J. molec. Spectrosc.*, **176**, 206.
[144] Li, M. G., and Coxon, J. A., 1996, *J. molec. Spectrosc.*, **180**, 287.
[145] Li, M. G., and Coxon, J. A., 1997, *J. molec. Spectrosc.*, **183**, 250.
[146] Li, M. G., and Coxon, J. A., 1997, *J. molec. Spectrosc.*, **184**, 395.
[147] Li, M. G., and Coxon, J. A., 1999, *J. molec. Spectrosc.*, **196**, 14.
[148] Elhanine, M., Lawruszczuk, R., and Soep, B., 1998, *Chem. Phys. Lett.*, **288**, 785.
[149] Greetham, G. M., and Ellis, A. M., 2001, *J. molec. Spectrosc.*, **206**, 198.
[150] Anticjovanovic, A., Bojovic, V., and Pesic, D., 1988, *Spectrosc. Lett.*, **21**, 757.
[151] Ni, Y., 1986, PhD Thesis, University of California, Santa Barbara.
[152] Li, M. G., and Coxon, J. A., 1992, *J. chem. Phys.*, **97**, 8961.
[153] Li, M. G., and Coxon, J. A., 1996, *J. chem. Phys.*, **104**, 4961.
[154] Li, M. G., and Coxon, J. A., 1994, *Can. J. Phys.*, **72**, 1200.
[155] Li, M. G., and Coxon, J. A., 1995 *J. chem. Phys.*, **102**, 2663.
[156] Presunka, P. I., and Coxon, J. A., 1995, *Chem. Phys.*, **190**, 97.
[157] Presunka, P. I., and Coxon, J. A., 1994, *J. chem. Phys.*, **101**, 201.
[158] Coxon, J. A., Li, M. G., and Presunka, P. I., 1994, *J. molec. Spectrosc.*, **164**, 118.
[159] Presunka, P. I., and Coxon, J. A., 1993, *Can. J. Chem.–Rev. Can. Chim.*, **71**, 1689.
[160] Coxon, J. A., Li, M. G., and Presunka, P. I., 1992, *Molec. Phys.*, **76**, 1463.
[161] Coxon, J. A., Li, M. G., and Presunka, P. I., 1991, *J. molec. Spectrosc.*, **150**, 33.
[162] Brazier, C. R., and Bernath, P. F., 1985, *J. molec. Spectrosc.*, **114**, 163.
[163] Bernath, P. F., and Kinseynielsen, S., 1984, *Chem. Phys. Lett.*, **105**, 663.
[164] Nakagawa, J., Wormsbecher, R. F., and Harris, D. O., 1983, *J. molec. Spectrosc.*, **97**, 37.
[165] Hilborn, R. C., Qingshi, Z., and Harris, D. O., 1983, *J. molec. Spectrosc.*, **97**, 73.
[166] Gustavsson, T., Alcaraz, C., Berlande, J., Cuvellier, J., Mestdagh, J. M., Meynadier, P., Depujo, P., Sublemontier, O., and Visticot, J. P., 1991, *J. molec. Spectrosc.*, **145**, 210.
[167] Fernando, W., Douay, M., and Bernath, P. F., 1990, *J. molec. Spectrosc.*, **144**, 344.
[168] Kinseynielsen, S., Brazier, C. R., and Bernath, P. F., 1986, *J. chem. Phys.*, **84**, 698.
[169] Jarman, C. N., and Bernath, P. F., 1992, *J. chem. Phys.*, **97**, 1711.

[170] O'Brien, L. C., and Bernath, P. F., 1986, *J. Am. chem. Soc.*, **108**, 5017.
[171] Cerny, T. M., Williamson, J. M., and Miller, T. A., 1995, *J. chem. Phys.*, **102**, 2372.
[172] Bopegedera, A., Fernando, W., and Bernath, P. F., 1990, *J. phys. Chem.*, **94**, 4476.
[173] Murphy, J. E., Berg, J. M., Merer, A. J., Harris, N. A., and Field, R. W., 1990, *Phys. Rev. Lett.*, **65**, 1861.
[174] Murphy, J. E., Friedmanhill, E., and Field, R. W., 1995, *J. chem. Phys.*, **103**, 6459.
[175] Li, J., Liu, Y. M., Moss, D. B., Gittins, C. M., Harris, N. A., and Field, R. W., 1999, *J. molec. Spectrosc.*, **193**, 403.
[176] Jakubek, Z. J., and Field, R. W., 1994, *Phys. Rev. Lett.*, **72**, 2167.
[177] Jakubek, Z. J., and Field, R. W., 1996, *J. molec. Spectrosc.*, **179**, 99.
[178] Jakubek, Z. J., and Field, R. W., 1997, *Phil. Trans. R. Soc.* A, **355**, 1507.
[179] Harris, N. A., and Field, R. W., 1993, *J. chem. Phys.*, **98**, 2642.
[180] Berg, J. M., Murphy, J. E., Harris, N. A., and Field, R. W., 1993, *Phys. Rev.* A, **48**, 3012.
[181] Huber, K. P., and Herzberg, G., 1979, *Molecular Spectra and Molecular Structure. IV. Constants of Diatomic Molecules* (New York: Van Nostrand Reinhold).
[182] Ernst, W. E., Kandler, J., Noda, C., McKillop, J. S., and Zare, R. N., 1986, *J. chem. Phys.*, **85**, 3735.
[183] Ernst, W. E., and Kandler, J., 1989, *Phys. Rev.* A, **39**, 1575.
[184] Gittins, C. M., Harris, N. A., Field, R. W., Verges, J., Effantin, C., Bernard, A., Dincan, J., Ernst, W. E., Bundgen, P., and Engles, B., 1993, *J. molec. Spectrosc.*, **161**, 303.
[185] Pereira, R., and Levy, D. H., 1996, *J. chem. Phys.*, **105**, 9733.
[186] Bolman, P. S. H., and Brown, J. M., 1973, *Chem. Phys Lett.*, **21**, 213.
[187] Pooley, S. J., Beardah, M. S., and Ellis, A. M., 1998, *J. Electron Spectrosc. Relat. Phenomena*, **97**, 77.
[188] Douay, M., and Bernath, P. F., 1990, *Chem. Phys. Lett.*, **174**, 230.
[189] Greetham, G. M., and Ellis, A. M., 2000, *Chem. Phys. Lett.*, **332**, 303.
[190] Vanvaals, J. J., Meerts, W. L., and Dymanus, A., 1984, *J. molec. Spectrosc.*, **106**, 280.
[191] Vanvaals, J. J., Meerts, W. L., and Dymanus, A., 1984, *Chem. Phys.*, **86**, 147.
[192] Vanvaals, J. J., Meerts, W. L., and Dymanus, A., 1983, *Chem. Phys.*, **82**, 385.
[193] Wormer, P. E. S., and Tennyson, J., 1981, *J. chem. Phys.*, **75**, 1245.
[194] Petrie, S., 1999, *Phys. Chem. chem. Phys.*, **1**, 2897.
[195] Brocks, G., 1987, *Chem. Phys.*, **116**, 33.
[196] Pasternack, L., and Dagdigian, P. J., 1976, *J. chem. Phys.*, **65**, 1320.
[197] Young, P. J., Gosavi, R. K., Connor, J., Strausz, O. P., and Gunning, H. E., 1973, *J. chem. Phys.*, **58**, 5280.
[198] Yu, C. F., Youngs, F., Tsukiyama, K., Bersohn, R., and Preses, J., 1986, *J chem. Phys.*, **85**, 1382.
[199] Jackson, R. L., 1990, *J. chem. Phys.*, **92**, 807.
[200] Jackson, R. L., 1992, *J. chem. Phys.*, **96**, 5938.
[201] Jackson, R. L., 1990, *Chem. Phys. Lett.*, **174**, 53.
[202] Blush, J. A., Chen, P., Wiedmann, R. T., and White, M. G., 1993, *J. chem. Phys.*, **98**, 3557.
[203] Jamorski, C., and Dargelos, A., 1992, *Chem. Phys.*, **164**, 191.
[204] Jamorski, C., Dargelos, A., Teichteil, C., and Daudey, J. P., 1993, *Chem. Phys.*, **178**, 39.
[205] Zakrzewski, V. G., and Ortiz, J. V., 1994, *J. chem. Phys.*, **100**, 6508.
[206] Karakyriakos, E., Davis, J. R., Wilson, C. J., Yates, S. A., McKinley, A. J., Knight, L. B., Babb, R., and Tyler, D. J., 1999, *J. chem. Phys.*, **110**, 3398.
[207] McKinley, A. J., Karakyriakos, E., Knight, L. B., Babb, R., and Williams, A., 2000, *J. phys. Chem.* A, **104**, 3528.
[208] Ellis, A. M., Robles, E. S. J., and Miller, T. A., 1992, *Chem. Phys. Lett.*, **190**, 599.
[209] Pooley, S. J., and Ellis, A. M., 1997, *J. molec. Spectrosc.*, **185**, 48.

[210] BEZANT, A. J., and ELLIS, A. M., 1997, *J. molec. Spectrosc.*, **185**, 54.
[211] FLOSS, F. P., and TRAEGER, J. C., 1975, *J. Am. chem. Soc.*, **97**, 1579.
[212] ZAKRZEWSKI, V. G., and ORTIZ, J. V., 1994, *J. phys. Chem.*, **98**, 13 198.
[213] LIE, J., and DAGDIGIAN, P., 2001, *J. chem. Phys.*, **114**, 2137.